1965

Partial molal heat capacities of some aqueous rare-earth chloride solutions at 25°C

Kenneth Cecil Jones
Iowa State University

PARTIAL MOLAL HEAT CAPACITIES OF SOME AQUEOUS RARE-EARTH CHLORIDE SOLUTIONS AT 25°C.

by

Kenneth Cecil Jones

A Dissertation Submitted to the
Graduate Faculty in Partial Fulfillment of
The Requirements for the Degree of
DOCTOR OF PHILOSOPHY

Major Subject: Physical Chemistry

Approved:

Signature was redacted for privacy.

In Charge of Major Work

Signature was redacted for privacy.

Head of Major Department

Signature was redacted for privacy.

Dean of Graduate College

Iowa State University
Of Science and Technology
Ames, Iowa

1965

TABLE OF CONTENTS

I. INTRODUCTION

Physical chemistry emerged as a separate scientific discipline in 1887 with the founding of the Zeitschrift für Physikalische Chemie, and for the first 30 years was largely concerned with studies of aqueous solutions. Today the study of solution properties constitutes only a small part of the domain of physical chemistry, but this does not mean that a complete understanding of solution behavior has been achieved. Indeed, one of the great challenges of physical chemistry at the present time is the development of an adequate theoretical interpretation of the properties of electrolytic solutions.

The interionic attraction theory of Debye and Hückel (1) is generally considered to give a satisfactory interpretation of very dilute electrolytic solutions. The limitation of the theory to dilute solutions is the result of certain simplifying assumptions in both the physical model and the mathematical treatment. Attempts to extend the range of applicability of the theory to higher concentrations by modifying one or more of the basic assumptions has generally been unsuccessful. It is now recognized that an adequate interpretation of concentrated solutions will require a knowledge of short range ion-ion and ion-solvent interactions and of the microscopic structure of the solution.

Perhaps the best approach for elucidating the complex nature of the electrolytic solutions is through a systematic

study of their thermodynamic properties. The thermodynamic method involves measurements of macroscopic observables, from which one tries to deduce the microscopic nature of the solution. The application of thermodynamic principles to solution phenomena was extensively developed by G. N. Lewis (2), and thermodynamic data have since provided a basis for our understanding of the nature of electrolytic solutions.

It is well known that the heat capacity of a given amount of water is greater than that of the same quantity of water which contains a small amount of a strong electrolyte. The presence of the ions affects the heat capacity of the water molecules to such an extent that their heat capacity is decreased by an amount greater than the intrinsic heat capacity of the ions. This behavior suggests that heat capacity data for concentrated solutions should provide a valuable insight into ion-solvent interactions. Moreover, heat capacity data are valuable in their own right, since they provide a means of calculating heats of dilution and activity coefficients at different temperatures. Although numerous investigations of heat capacities of solutions of uni-univalent electrolytes have been conducted, comparatively few such measurements have been made on solutions of polyvalent electrolytes.

The rare-earth elements form a number of salts which offer several unique advantages for experimental and theoretical studies of electrolytic solutions. The true rare earths

are the group of elements in the periodic table beginning with cerium (atomic number 58) and ending with lutetium (atomic number 71). However, because lanthanum exhibits chemical properties very similar to those of the true rare earths, we shall consider it to be a rare-earth element also. Owing to their unique electronic configurations, the rare earths exist in aqueous solution as trivalent ions and possess remarkably similar chemical properties. As the nuclear charge increases with increasing atomic number, electrons are added to the inner 4f subshell which is well shielded by the completed 5s and 5p subshells. Because of this shielding, the 4f electrons have almost no influence on the chemical properties of these elements, which instead are determined by three outer valence electrons common to all rare-earth elements. In addition, as the nuclear charge increases, the outer electron shells are pulled in closer to the nucleus, resulting in the gradual decrease in atomic radius across the series known as the "lanthanide contraction". For this reason the rare earths provide an ideal series for studying the effect of a change in ionic radius on solution properties while maintaining the ionic charge constant. Other advantages of the rare earths relative to other polyvalent cations are the following: they form a large number of salts which are soluble in water over a wide concentration range; their degree of hydrolysis is small and can be readily controlled; and their tendency to form complexes with simple anions in aqueous solutions is generally

slight at low concentrations.

Until about 1950, the rare earths were not widely available in sufficient quantity or purity to allow an extensive investigation of their solution properties. However, shortly after the development of large-scale ion exchange separation methods at the Ames Laboratory (3), the rare earths became commercially available in large quantities and high purity. As a result, an extensive program was initiated in this laboratory to obtain precise thermodynamic and transport data for rare-earth salt solutions. The work up to 1959 has been reviewed by Spedding and Atkinson (4), and they noted definite differences in the solution properties of rare-earth salts. Although these differences were small, they were not the simple monotonic functions of ionic radius one might expect. Later work on apparent molal volumes (5) and relative apparent molal enthalpies (6,7) of rare-earth chloride solutions indicated that a change in coordination number of the rare-earth ions occurred near the middle of the series.

With these considerations in mind, it seemed advisable to investigate the behavior of concentrated rare-earth chloride solutions through a study of their heat capacities. Specific heats of lanthanum, neodymium, dysprosium, erbium, and ytterbium chloride solutions were determined at 25°C. over the concentration range 0.1 molal to saturation. The salts were chosen from opposite ends of the rare-earth series to provide a means of testing the hypothesis that different coordination numbers exist for the light and heavy rare earths.

II. THERMODYNAMIC INTRODUCTION

A. Fundamental Concepts and Definitions

Thermodynamics is an exact science concerned with the description of macroscopic properties of systems of interest. The thermodynamic states of a system can be completely described by means of certain variables which depend only on the state of the system and not on the path by which the state is reached. Such variables are called thermodynamic state functions.

Consider a system of constant mass which undergoes a change from one equilibrium state to another. The first law of thermodynamics requires that the change in energy of the system depends only on the initial and final states of the system, and not on the path by which the change occurs. The energy E, is therefore a state function. Mathematically, the first law is given by

$$\Delta E = E_f - E_i = Q - W \qquad (2.1)$$

where Q is the heat absorbed by the system from its surroundings, W is the work done by the system on its surroundings, and the subscripts i and f refer to the initial and final states respectively. The convention followed here is that Q is positive when the system absorbs heat from the surroundings and W is positive when the system does work on the surroundings. Although ΔE is independent of the path, both Q and W depend on the path by which the change in state occurs; hence, heat and work are not state functions.

For a process in which all work is excluded except pressure-volume work, Equation 2.1 may be written as

$$\Delta E = Q - P\Delta V, \qquad (2.2)$$

where P is the pressure and V is the volume. If the process is also conducted at constant volume, $\Delta V = 0$, and

$$\Delta E = Q_V, \qquad (2.3)$$

where Q_V is the heat absorbed at constant volume. Instead, if the process is performed at constant pressure, Equation 2.2 may be written as

$$\begin{aligned} Q_p &= \Delta E + P\Delta V \\ &= (E_f + PV_f) - (E_i + PV_i), \end{aligned} \qquad (2.4)$$

where Q_p is the heat absorbed at constant pressure. Since E, P, and V are state functions, we may define another state function H, called the enthalpy, by the relation

$$H = E + PV . \qquad (2.5)$$

Equation 2.4 then becomes

$$Q_p = \Delta H . \qquad (2.6)$$

When a system absorbs a quantity of heat Q, and undergoes a change of temperature from T_i to T_f, the average heat capacity is given by the ratio

$$C(\text{ave}) = \frac{Q}{T_f - T_i} . \qquad (2.7)$$

The true heat capacity of the system is obtained from the limit of this ratio as the temperature interval approaches zero, thus:

$$C = \underset{(T_f \to T_i)}{\text{limit}} \frac{Q}{T_f - T_i} = \frac{dQ}{dT} . \qquad (2.8)$$

The heat capacity defined by either of these expressions has a definite value only for a specified process because Q is not a state function. Moreover, the average heat capacity for a certain process will depend on the precise temperature interval chosen. To avoid the ambiguity caused by the choice of interval, the definition of heat capacity by Equation 2.8 is preferred. In many cases, as is true in this work, it is possible to choose a small finite temperature interval such that the difference between the average and true heat capacities is negligible.

Suppose we specify a process in which the volume is maintained constant. Then from Equations 2.3 and 2.8 we have

$$C_V = \frac{dQ_V}{dT} = \left(\frac{\partial E}{\partial T}\right)_V , \qquad (2.9)$$

where C_V is the heat capacity for the constant volume process. Similarly, for a constant pressure process, we may combine Equations 2.6 and 2.8 and write

$$C_p = \frac{dQ_p}{dT} = \left(\frac{\partial H}{\partial T}\right)_p , \qquad (2.10)$$

where C_p is the corresponding heat capacity for the constant pressure process. Heat capacities given by Equations 2.9 and 2.10 are state functions for the specified processes. Throughout this report, the term "heat capacity" will refer to a constant pressure process, and "specific heat" to the

heat capacity at constant pressure per unit weight of material.

B. Partial Molal Quantities

Thermodynamic state functions may be grouped into two classes: intensive and extensive. An intensive variable is one which has the same magnitude regardless of the amount of material chosen. Temperature, pressure, and specific heat are examples of intensive variables. The magnitude of an extensive variable is proportional to the amount of material under consideration; examples are volume, energy, heat capacity, and number of moles.

Extensive variables possess the mathematical property of being homogeneous functions of degree one. A function $f(x_1, x_2, \ldots x_k)$ is said to be homogeneous of degree n in the variables $x_1, x_2, \ldots x_k$ if

$$f(bx_1, bx_2, \ldots bx_k) = b^n f(x_1, x_2, \ldots x_k) \qquad (2.11)$$

for all positive values of b. If the degree of homogeneity is one, multiplication of each of the independent variables by b is equivalent to multiplying the over-all function by the same factor. For any positively homogeneous function, Euler's theorem states that

$$\sum_{i=1}^{k} x_i \left(\frac{\partial f}{\partial x_i} \right) = nf(x_1, x_2, \ldots x_k) \; . \qquad (2.12)$$

Let Y be any extensive thermodynamic property of a multicomponent system. Then Y can be expressed as a function of the independent variables temperature, pressure, and number of

moles of each component, i.e.,

$$Y = Y(T,P,n_1,n_2,\ldots n_k) \quad . \tag{2.13}$$

Applying Equation 2.12 to the extensive variables $n_1,n_2,\ldots n_k$, while holding the intensive variables T and P constant, we obtain

$$Y = \sum_{i=1}^{k} n_i \left(\frac{\partial Y}{\partial n_i}\right)_{T,P,n_j} \quad , \tag{2.14}$$

where the subscripts T, P, and n_j indicate the variables held constant during the partial differentiations. n_j represents the number of moles of all components except component i.

For every extensive variable Y, we define a corresponding intensive variable $\bar{Y}_i$, called the partial molal quantity of component i, by the relation

$$\bar{Y}_i = \left(\frac{\partial Y}{\partial n_i}\right)_{T,P,n_j} \quad . \tag{2.15}$$

From this definition, Equation 2.14 for a two component system becomes

$$Y = n_1\bar{Y}_1 + n_2\bar{Y}_2 \quad . \tag{2.16}$$

Another useful function is the apparent molal quantity of component 2, ϕ_Y, which is defined by

$$\phi_Y = \frac{Y - n_1\bar{Y}_1^o}{n_2} \quad , \tag{2.17}$$

where $\bar{Y}_1^o$ is the partial molal quantity of component 1 in an arbitrary reference state.

Since the heat capacity at constant pressure is an extensive thermodynamic variable, we can write Equations 2.16 and 2.17 as

$$C_p = n_1\bar{C}_{p1} + n_2\bar{C}_{p2} \tag{2.18}$$

and

$$C_p = n_1 \bar{C}^o_{p1} + n_2 \phi_{cp} \quad . \tag{2.19}$$

Throughout this report, the subscripts 1 and 2 refer to the solvent and solute respectively. Hence, for an aqueous solution, $\bar{C}^o_{p1}$ is the molal heat capacity of pure water, the arbitrary reference state being taken as infinite dilution ($n_2 = 0$). It follows from Equations 2.18 and 2.19, that at infinite dilution $\bar{C}^o_{p2} = \phi^o_{cp}$. Differentiation of Equation 2.19 with respect to n_2, holding n_1 constant, yields

$$\left(\frac{\partial C_p}{\partial n_2}\right)_{n_1} = \bar{C}_{p2} = \phi_{cp} + n_2 \left(\frac{\partial \phi_{cp}}{\partial n_2}\right)_{n_1} . \tag{2.20}$$

Combining Equations 2.18 and 2.19 gives

$$\bar{C}_{p1} = \bar{C}^o_{p1} + \frac{n_2}{n_1} (\phi_{cp} - \bar{C}_{p2}) \quad , \tag{2.21}$$

and substituting the value for $\bar{C}_{p2}$ from Equation 2.20, we obtain

$$\bar{C}_{p1} = \bar{C}^o_{p1} - \frac{n_2^2}{n_1} \left(\frac{\partial \phi_{cp}}{\partial n_2}\right)_{n_1} . \tag{2.22}$$

Since ϕ_{cp} is often conveniently expressed as an analytic function of $m^{\frac{1}{2}}$, where m is the number of moles of solute per 1000 grams of solvent, it is desirable to represent $\bar{C}_{p1}$ and $\bar{C}_{p2}$ as functions of $m^{\frac{1}{2}}$. Employing the relations

$$n_1 = 1000/M_1 \quad , \tag{2.23}$$

where M_1 is the molecular weight of water, and

$$n_2 = (m^{\frac{1}{2}})^2 \quad , \tag{2.24}$$

Equations 2.20 and 2.22 become

$$\bar{C}_{p2} = \phi_{cp} + \tfrac{1}{2} m^{\frac{1}{2}} \left(\frac{\partial \phi_{cp}}{\partial m^{\frac{1}{2}}}\right) \tag{2.25}$$

and

$$\bar{C}_{p1} = \bar{C}^{o}_{p1} - \frac{M_1}{2000} m^{3/2} \left(\frac{\partial \phi_{cp}}{\partial m^{\frac{1}{2}}} \right) . \qquad (2.26)$$

The apparent molal heat capacity is related to the specific heat by the expression

$$\phi_{cp} = (\frac{1000}{m} + M_2)s - \frac{1000}{m} s^{o} , \qquad (2.27)$$

where m is the molality of the solute of molecular weight M_2, and s and s^{o} are the specific heats of the solution and pure water respectively. Consequently, evaluation of the apparent and partial molal heat capacities reduces to a determination of specific heats of the solutions.

III. HISTORICAL REVIEW

A. Electrolytic Solution Theory

The origin of the modern theory of electrolytic solutions dates back to 1887 when Arrhenius (8) postulated his now famous dissociation theory. He proposed that all electrolytes in aqueous solution were partially dissociated into ions which did not interact, and that an equilibrium existed between these ions and the undissociated solute molecules. He further proposed that the degree of dissociation increased upon dilution and was complete only at extreme dilution. Prior to this time, the prevailing attitude was that the number of free ions in solution at any concentration was infinitesimal. Acceptance of the Arrhenius theory was due in large measure to its ability to explain the colligative properties of electrolytic solutions, particularly the osmotic pressure studies of van't Hoff (9).

Although the Arrhenius theory was moderately successful for weak electrolytes, the behavior of strong electrolytes presented many anomalies. Values of the dissociation constant obtained from conductivity ratios were not in agreement with those from osmotic pressure studies, and often values were obtained which were greater than unity. In addition, the Arrhenius theory assumed the ionic mobilities to be independent of concentration for all electrolytes, which was not in agreement with the observed concentration dependence of

transference numbers. Finally, two striking arguments for complete dissociation of strong electrolytes were provided by the ionic structure of crystalline salts and the failure of absorption spectra of solutions of strong electrolytes to show any evidence of undissociated molecules.

Perhaps the major criticism of the Arrhenius theory was its failure to consider the electrostatic interaction between ions in solution. As early as 1894, van Laar (10) emphasized the importance of electrostatic forces in explaining the behavior of ionic solutions. Sutherland (11,12) and Bjerrum (13) were among the first to adopt the view that the behavior of strong electrolytes in solution could be accounted for on the basis of complete dissociation and by an adequate consideration of the effects of ionic interactions. Several unsuccessful attempts were made to calculate the effect of these ionic interactions before Milner (14,15) in 1912 successfully analyzed the problem. He showed that deviations from ideality of electrolytic solutions could be calculated from the interionic Coulomb forces. Unfortunately, his calculation was too involved to be of any practical value.

The first practical theoretical treatment of solutions of strong electrolytes was presented by Debye and Hückel (1) in 1923. By introducing the concent of an ionic "atmosphere", and through application of Poisson's equation of electrostatics and the Boltzman distribution function, they derived a limiting expression for the activity coefficient. The basic

assumptions employed in the Debye-Hückel theory are the following:

1. Strong electrolytes in solution are completely dissociated into ions.
2. Deviations from ideality are ascribed entirely to Coulombic interactions of the ions.
3. The ions are hard spheres with a mean distance of closest approach.
4. The solvent is a continuous medium with a uniform dielectric constant.
5. In the absence of external fields, any given ion is surrounded by a symmetrical distribution of ions, containing on the average more ions of unlike charge than like charge. The time average distribution of this ionic "atmosphere" is given by the Boltzman distribution function.
6. The electrostatic potential at any point in the solution can be calculated from the Poisson equation using a form of the Boltzman distribution function which is compatible with the principle of linear superposition of fields. This requires that the Boltzman function be expanded as a power series, and terms of higher order than the first be neglected.

Using these assumptions, Debye and Hückel were able to formulate the following expression for the mean rational activity coefficient:

$$\log f_{\pm} = - \frac{\phi_f \sqrt{I}}{1 + a^o B \sqrt{I}} \qquad (3.1)$$

with

$$\phi_f = \frac{1}{2.303} \frac{1}{\nu} \sum_i \nu_i z_i^2 \left(\frac{\pi N e^6}{1000 (DkT)^3} \right)^{\frac{1}{2}} ,$$

$$B = \left(\frac{4\pi N e^2}{1000 DkT} \right)^{\frac{1}{2}}$$

and

$$I = \sum_i c_i z_i^2 .$$

Here, I is the ional concentration; ν, the number of ions produced by the dissociation of one molecule of electrolyte of which ν_i ions have a charge z_i; c_i, the concentration in moles per liter of the i-type ions; N, Avogadro's number; k, the Boltzman constant; e, the electronic charge; D, the dielectric constant of the solvent; T, the absolute temperature; and a^o, the mean distance of closest approach of the ions.

Equation 3.1 has been found to agree well with experiment at concentrations up to I = 0.1 if a^o is used as an adjustable parameter. Since no straightforward correlation has been found between the a^o values used and crystallographic radii, it is considered to be a parameter which corrects for imperfections in the theory.

In the limit of infinite dilution, the quantity $a^o B \sqrt{I}$ becomes small compared to unity, and Equation 3.1 reduces to the Debye-Hückel limiting law,

$$\log f_{\pm} = -\phi_f \sqrt{I} . \qquad (3.2)$$

For a solution containing a single electrolyte, the ional concentration is related to the molar concentration c, by

$$I = c \sum_i \nu_i z_i^2 , \qquad (3.3)$$

and the limiting law may be written as

$$\log f_\pm = -S_f \sqrt{c} \qquad (3.4)$$

where

$$S_f = \mathcal{S}_f \left[\sum_i \nu_i z_i^2 \right]^{\frac{1}{2}} . \qquad (3.5)$$

The statistical-mechanical foundations of the Debye-Hückel theory have been subjected to close scrutiny by a number of authors (16,17,18,19,20,21). These examinations, in conjunction with numerous experimental investigations, provide convincing arguments for the validity of the theory in the limit of high dilutions. For a detailed treatment of the Debye-Hückel theory, the monograph of Harned and Owen (22) or the treatise of Robinson and Stokes (23) should be consulted.

With the success of the Debye-Hückel theory in describing the behavior of dilute solutions of strong electrolytes, attention was directed to more concentrated solutions. Attempts to extend its range of applicability by considering such factors as ion-association (24,25,26), ion-solvent interactions (27, 28,29,30), and deviations from the Boltzman distribution function (31,32,33,34) have had only limited success. Such methods generally yield expressions containing additional parameters which are incapable of independent evaluation or precise physical interpretation. Furthermore, since the

temperature and pressure dependence of these parameters is generally unknown, the extended forms are of little use in interpreting heat capacity, enthalpy, or volume data.

A somewhat different approach was taken by Mayer (35). He adapted his cluster sum theory of imperfect gases to electrolytic solutions and succeeded in obtaining an expression for the activity coefficient. His result is consistent with the Debye-Huckel theory, but as Poirier (36) has shown, is similarly restricted to dilute solutions.

B. Heat Capacities - Comparison of Theory With Experiment

Publication of the Debye-Hückel theory stimulated interest in experimental studies of heat capacities of solutions. In 1927 Randall and Ramage (37) observed that the apparent molal heat capacities of sodium chloride and hydrochloric acid were linear functions of the square root of concentration up to about two molal. Several years later, Randall and Rossini (38) obtained very accurate heat capacity data for a number of solutions of strong electrolytes using a differential calorimeter. Their results, and those of subsequent investigators (39,40,41), confirmed the observation of Randall and Ramage. Rossini (42) tabulated the available data for uni-univalent electrolytes and found the linear relationship between the apparent molal heat capacity and the square root of concentration to be valid up to 2.5 molal.

The Debye-Hückel theory predicts a linear variation of

the apparent molal heat capacity with the square root of concentration in dilute solutions. From the limiting law, Equation 3.4, and the thermodynamic relationship between the partial molal heat capacity and the activity coefficient,

$$\bar{C}_{p2} - \bar{C}^{o}_{p2} = -\nu R \frac{\partial}{\partial T}\left[T^2 \frac{\partial \ln f_{\pm}}{\partial T}\right], \qquad (3.6)$$

LaMer and Cowperthwaite (43) showed that

$$\bar{C}_{p2} - \bar{C}^{o}_{p2} = S_{cp}\sqrt{c} \quad . \qquad (3.7)$$

The limiting slope for the partial molal heat capacity is given by

$$S_{cp} = 2.303\,\nu R\,\phi_f\,F(D,V,T) \qquad (3.8$$

where R is the gas constant and

$$F(D,V,T) = 3/4\left\{1 + 2\frac{T}{D}\frac{\partial D}{\partial T} + 5\left(\frac{T}{D}\frac{\partial D}{\partial T}\right)^2 + \frac{2T^2}{DV}\frac{\partial D}{\partial T}\frac{\partial V}{\partial T} + \frac{2T}{3V}\frac{\partial V}{\partial T} + \left(\frac{T}{V}\frac{\partial V}{\partial T}\right)^2 - \frac{2T^2}{D}\frac{\partial^2 D}{\partial T^2} - \frac{2}{3}\frac{T^2}{V}\frac{\partial^2 V}{\partial T^2}\right\} . \qquad (3.9)$$

For high dilutions, the molar concentration c, may be replaced by $d_o m$, where d_o is the density of the pure solvent and m is the molal concentration. Hence, Equation 3.7 becomes

$$\bar{C}_{p2} - \bar{C}^{o}_{p2} = \sqrt{d_o}\,S_{cp}\sqrt{m} \quad . \qquad (3.10)$$

It follows from Equations 3.10 and 2.25 that

$$\phi_{cp} - \phi^{o}_{cp} = 2/3\sqrt{d_o}S_{cp}\sqrt{m} \quad . \qquad (3.11)$$

Although ϕ_{cp} is often observed to be a linear function of $m^{\frac{1}{2}}$ over a wide concentration range, this does not constitute a verification of the Debye-Hückel theory because the limiting law cannot be expected to hold in any but the most dilute

solutions.

The experimental limiting slopes of the uni-univalent electrolytes tabulated by Rossini differ widely among themselves and from the theoretical limiting slope. Young and Machin (44) pointed out that if the differences were significant, the data were in conflict with the Debye-Hückel theory which demands the same limiting slope for all strong electrolytes of the same valence type. They investigated the validity of using a linear extrapolation of apparent molal heat capacity data to determine the limiting slope of sodium chloride. Their results, obtained from heat of dilution measurements at two temperatures, showed a rapid change in slope of the ϕ_{cp} vs. $m^{\frac{1}{2}}$ curve below 0.2 molal. They concluded the slope was changing so rapidly near the origin that a limiting slope determined by a linear extrapolation from moderate concentrations was not valid, and therefore differences between limiting slopes of various salts of the same valence type were not significant and did not constitute evidence of failure of the theory.

Precise data for higher valence salts are very limited, but in general, the simple linear variation of ϕ_{cp} with $m^{\frac{1}{2}}$ is not followed, even at moderate concentrations. LaMer and Cowperthwaite (43) studied very dilute solutions of zinc sulfate and found appreciable deviation from linearity even as low as 0.0005 molal. Wallace and Robinson (45) found a definite change in slope for sodium sulfate below 0.04 molal

and a limiting slope which agreed with theory. Later they reported results for cadmium chloride, bromide, and iodide (46) in which ϕ_{cp} was far from a linear function of $m^{\frac{1}{2}}$ at higher concentrations. This behavior was attributed to ion-association. Spedding and Miller (47) reported limiting slopes for neodymium and cerium chlorides which were in good agreement with theory. Within the uncertainty of their data, ϕ_{cp} was found to be a linear function of $m^{\frac{1}{2}}$ up to 0.36 molal, the highest concentration studied.

In view of the success of the Debye-Hückel theory in predicting the behavior of activity coefficients and partial molal enthalpies in dilute solutions, one has every confidence in the limiting equation for partial molal heat capacities. Unfortunately, as Gucker and Schminke (39) pointed out, even for the most accurate specific heat data, the uncertainty in the apparent molal heat capacity becomes very large at high dilutions. As a result, applicability of heat capacity measurements for testing the validity of the Debye-Hückel theory is indeed questionable. Furthermore, uncertainties in the first and second temperature derivatives of the dielectric constant of water, impart a considerable uncertainty in the theoretical limiting slope.

In addition to the approach of Debye and Hückel, several other theoretical attempts have been made to describe the behavior of heat capacities of solutions of strong electrolytes. Zwicky (48,49,50) treated electrolytic solutions from

the standpoint of water under high pressure and was able to predict the order of magnitude of $\bar{C}^{o}_{p2}$. His theory has been criticized for its failure to predict a linear relationship between ϕ_{cp} and $m^{\frac{1}{2}}$ (51). Everett and Coulson (52) applied statistical mechanics to the calculation of ionic heat capacities by considering the influence of ions on the freedom of rotation of water molecules in the first hydration shell of the ions. Their treatment was severely restricted because of a lack of knowledge of the species present in solution. Such theoretical approaches at best give only a qualitative understanding of heat capacities of electrolytic solutions because they are unable to account for specific differences observed experimentally.

At the present time, one of the major unsolved problems of physical chemistry is the lack of an adequate theoretical description of concentrated solutions. The difficulties in the development of such a theory can be appreciated when one realizes that in addition to the long-range ionic interactions treated by Debye and Hückel, short-range effects such as ion-association and ion-solvent interactions must also be considered. The size and charge of the ions, and their affect of the dielectric constant and structure of the solvent must be included. Development of an experimental method which could precisely determine the species present in a solution would certainly be very useful. Perhaps, as Fuoss and Onsager (53)

have suggested, the final theory of electrolytic solutions will proceed from a projection of a theory of fused salts into the region of concentrated solutions.

IV. EXPERIMENTAL

A. Description of the Calorimeter

The choice of a calorimeter design is dependent on the particular problem to be studied and the degree of accuracy desired. Numerous calorimeters have been built to meet the requirements of a variety of thermochemical problems. White (54), Swietoslawski (55), Sturtevant (56), and Skinner (57) have discussed the construction, operation, and applications of many types of calorimeters.

The calorimeter which was designed and built for this research was an adiabatically controlled, single vessel type and is shown schematically in Figure 1. It was capable of providing specific heat data for aqueous solutions with a precision of better than 0.05% in the temperature range from 24.0 to 26.0°C. The calorimeter vessel is shown in detail in Figure 2. References to the figures will be designated by (n-X) where n refers to the figure number and X to the alphabetically labeled part.

The apparatus consisted of a calorimeter vessel (1-D) suspended in an evacuated submarine jacket (1-E) which was submerged in a well stirred water bath (1-C). The operational components consisted of a vacuum system, systems for the measurement of temperature and electrical energy, and a system for adiabatic control of the bath.

Heat transfer between the calorimeter and its surroundings was minimized by evacuation of the submarine jacket and

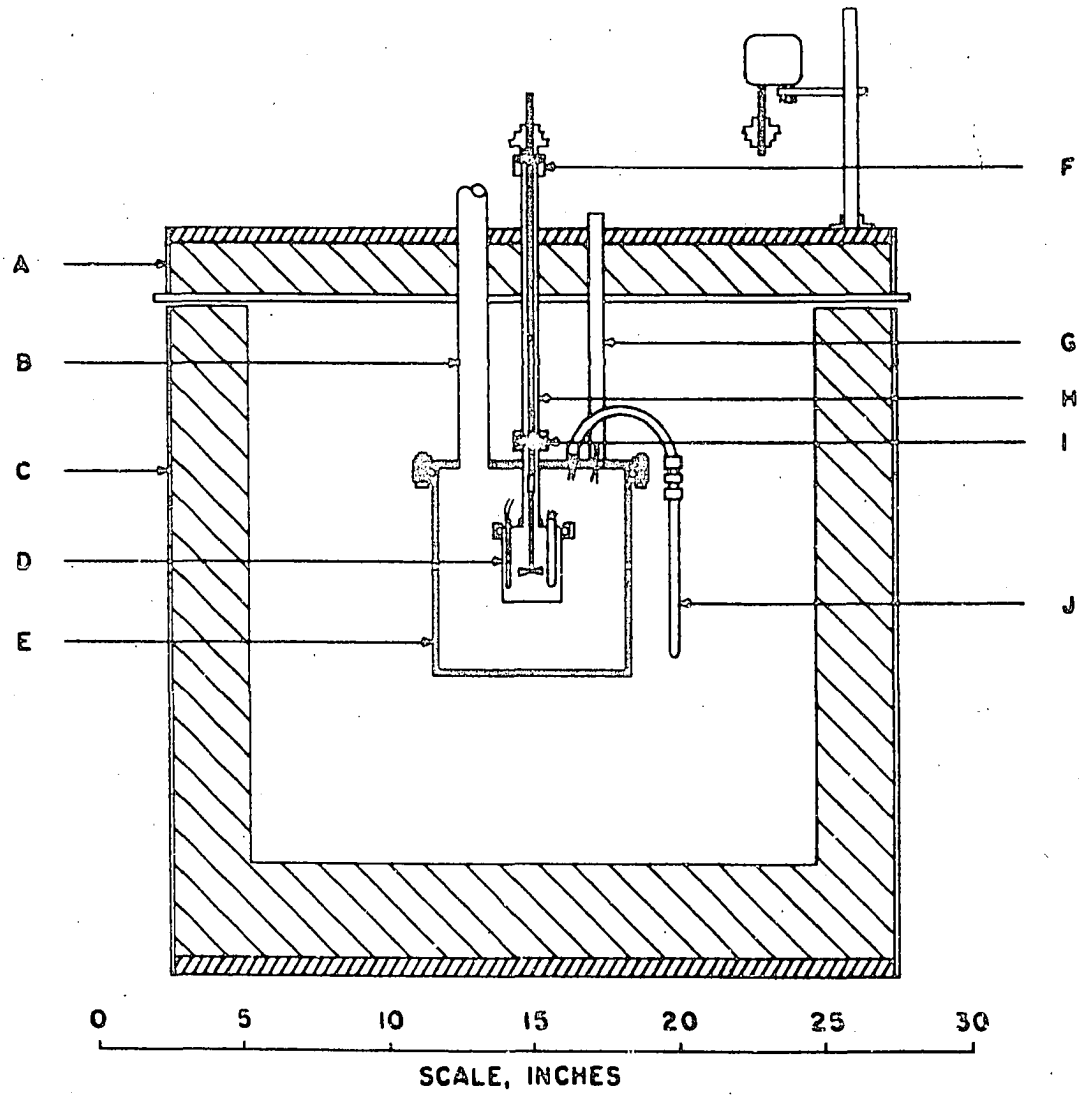

Figure 1. Adiabatic solution calorimeter

carefully controlling the bath temperature so as to maintain a very small temperature differential between the calorimeter and the bath. In this way, essentially adiabatic conditions were maintained. A multijunction thermopile between the calorimeter and the bath served as a differential temperature sensing device.

The calorimeter temperature was measured with a thermistor thermometer in a normal Wheatstone bridge circuit and continuously recorded. The following precautions were taken to ensure reproducible temperature measurements: the current in the thermistor was maintained nearly constant and at such a level that self heating was negligible; once energized, the power was never removed from the thermistor; the thermistor was rigidly mounted and never subjected to mechanical or thermal shocks.

In the past ten years, thermistors have gained wide acceptance as calorimeter thermometers (58,59,60,61) because of their small size, rapid response, and high sensitivity. Thermistors are ceramic-like semi-conductors with large negative temperature coefficients of resistance. They are made by sintering mixtures of metallic oxides; manganese, nickel, cobalt, and iron being the most commonly used.

With this general description of the adiabatic calorimeter, we will now consider in detail each of the components of the apparatus.

1. Water bath

The water bath (1-C), which served as the adiabatic jacket of the calorimeter, was a double-walled tank with a capacity of 22 gallons. A three inch space between the inner and outer walls of the bath was filled with exploded mica for insulation. The bath was mounted on a movable carriage and could be raised and lowered by a hydraulic bumper jack. With the bath in its lowered position, the carriage could be moved aside to facilitate assembly of the calorimeter vessel and submarine jacket. A lid (1-A) for the bath was suspended 55 inches above the floor on an angle iron frame. It was also double-walled with insulation filling the three inch space between the walls.

A centrifigual stirrer (Central Scientific Company catalog number 18850), with a rated capacity of 100 gallons per minute was used to stir the water in the bath. It was mounted on the lower face of the bath lid. This stirrer was found to give very satisfactory mixing of the water with a minimum of heating. A smaller centrifigual pump was originally used and found to be unsatisfactory because too much heat was generated by friction of the impeller against its housing.

For control purposes, the bath was equipped with a cooling coil and two heaters. Cooling was accomplished by allowing cold water to flow continuously through two turns of copper tubing near the bottom of the bath. The control heater was a centrally located, 500 watt calrod. A 750 watt calrod was located near the bottom of the bath and served as an

auxilliary heater. Control of the bath will be described in a later section.

2. Submarine jacket

The submarine jacket (1-E) was a cylindrical monel can, 6 1/2 inches in diameter and 6 1/2 inches deep. The sides were 1/16 inch thick and the bottom 1/8 inch thick. A brass collar, machined to house a 6 1/2 by 1/8 inch O-ring, was silver soldered to the top lip of the jacket. Eight stainless steel studs were screwed into the collar and used to fasten the submarine jacket to its lid, which was a quarter inch thick monel disk, 7 1/2 inches in diameter. The submarine lid was suspended from the water bath lid by three, half inch diameter brass pipes (only two are shown in Figure 1). Each pipe was silver soldered to the submarine lid. Two of these pipes (1-G) served as conduits for the shielded electrical cables entering the submarine, and the other (1-H) housed the calorimeter stirring shaft. All electrical leads entered the submarine lid through vacuum tight seals.

3. Vacuum system

The submarine jacket was evacuated through a one inch copper tube (1-B), which was attached to a 25 mm. glass vacuum line by means of a glass to metal seal. A mechanical fore-pump was used in conjunction with an oil diffusion pump to obtain a pressure of the order of 1×10^{-5} torr. The pressure was measured with an ionization gauge. A liquid nitrogen cold trap prevented oil vapors from entering the vacuum line.

In order to obtain a vacuum tight system, all joints were welded or silver soldered wherever possible. However, because of the diversity of materials used in the construction of the calorimeter vessel, this was not always possible. In these instances, vacuum seals were obtained with Torr Seal, a low vapor pressure epoxy resin obtained from Varian Associates.

4. Calorimeter vessel

The calorimeter vessel and lid were constructed from 20 mil tantalum to insure chemical inertness and mechanical strength. The vessel (1-D, 2-C) was two inches in diameter by 2 1/2 inches deep and had a volume of 110 ml. Tantalum wells were welded into the lid to house the heater (2-D), thermometer (2-G), and thermopile (2-H). An aluminum ring, machined to house a 2 1/8 by 1/8 inch O-ring, was attached with Torr Seal to the outside upper lip of the vessel. This ring did not come in contact with the solution.

The calorimeter lid was suspended two inches below the submarine lid by a half inch diameter, thin wall (0.006 inch), stainless steel hanger (2-A). At its upper end, the hanger was silver soldered to the submarine lid, and at its lower end, to a threaded brass flange. The calorimeter lid was attached to the hanger with a threaded lug, which screwed into the brass flange.

The calorimeter vessel was attached to its lid with a threaded cap and collar arrangement. A brass cap was attached with Torr Seal to the top, outer edge of the tantalum lid.

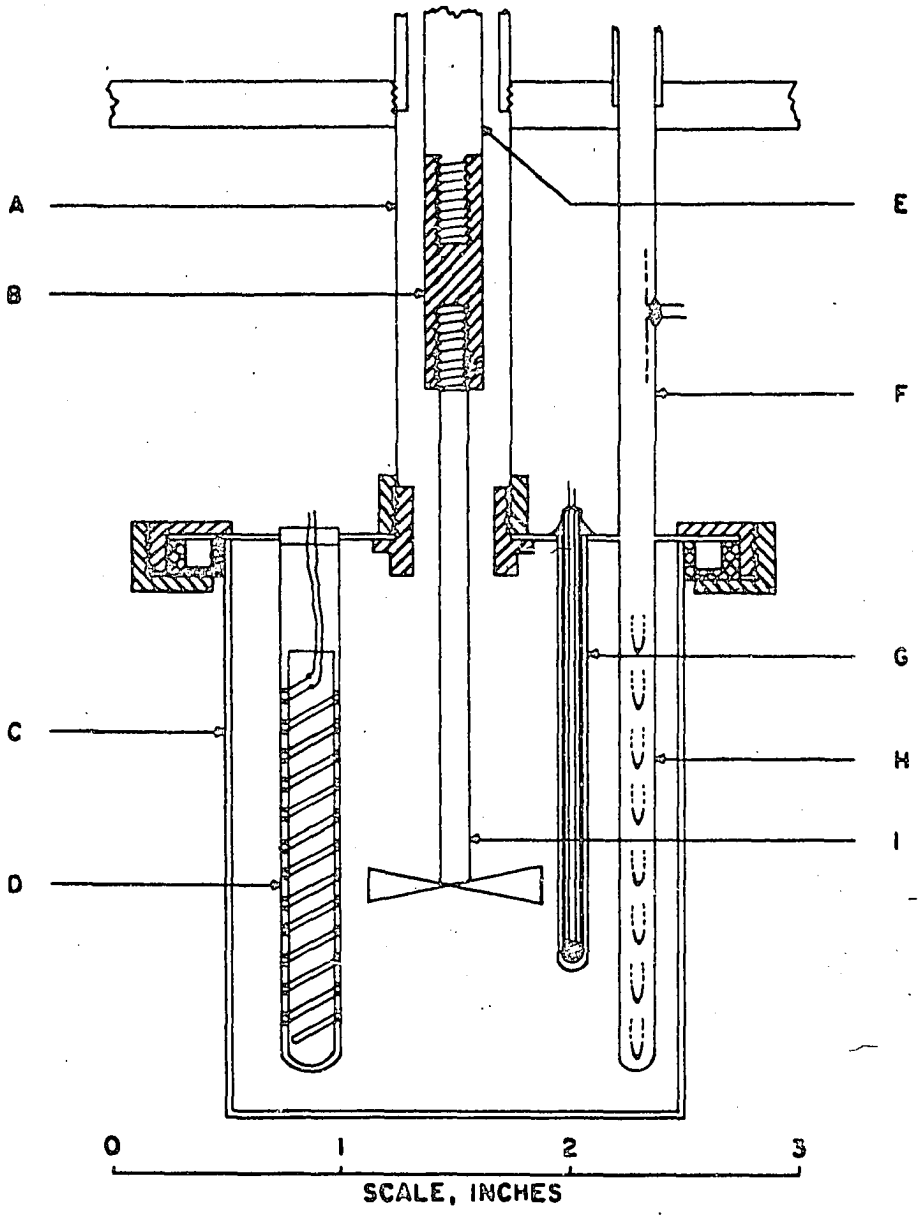

Figure 2. Calorimeter vessel

The brass collar fit freely over the outside of the vessel and when screwed onto its matching cap, compressed the O-ring against the tantalum lid. This gave a vacuum tight connection which was easily assembled. A disadvantage of this type of assembly was that it was slow to equilibrate to the solution temperature. This problem has been discussed by Sunner and Wadsö (61).

5. Stirrer

The solution in the calorimeter vessel was stirred by a four blade tantalum propeller attached to a 1/8 inch diameter tantalum shaft (2-I). The upper end of the tantalum shaft was screwed into a polystyrene thermal insulator (2-B), which in turn was screwed into a quarter inch diameter stainless steel shaft (2-E). The polystyrene insulator helped reduce conduction of heat from the bearings into the calorimeter.

The stainless steel stirring shaft was held in place by two bearings; one located about an inch above the submarine lid (1-I), and another the same distance above the water bath lid (1-F). A 300 rpm synchronous motor provided the power to drive the stirrer. Two cone pulleys, one on the motor and the other on the stirring shaft, were coupled by a rubber O-ring. Each cone pulley had three steps, giving a total of six possible stirring speeds from 140 to 320 rpm. This variation in speeds made it possible to control the energy input due to stirring as the viscosities of the solutions changed.

6. Thermometer

The thermometer circuit was a standard Wheatstone bridge arrangement and is shown in Figure 3. The temperature sensing element in the bridge was a glass probe type thermistor (Fenwall number G463), with a nominal resistance of 110,000 ohms at 25°C. It was housed in a tantalum well (2-G) in the calorimeter to provide protection against breakage. Each of the ratio arms of the bridge contained a 100,000 ohm wire-wound resistor. The balancing arm consisted of a 105,000 ohm wire-wound resistor in series with a 10,000 ohm decade box, variable in steps of one ohm. Settings on the decade box corresponded to temperatures between 24.0 and 26.0°C. Power was supplied to the bridge by a 1.35 volt mercury cell which was never removed from the circuit. Under these conditions, the current through the thermistor was about six microamperes. The off-balance signal from the bridge was amplified 240 times and displayed on a ten millivolt strip-chart recorder. A one millimeter displacement of the recorder pen corresponded to a change in resistance of the thermistor of about 0.1 ohm, which was equivalent to a temperature change of 2×10^{-5}°C.

The thermistor bridge was calibrated in the following way. A platinum resistance thermometer, previously calibrated by the National Bureau of Standards, was inserted into the calorimeter near the thermistor. The calorimeter temperature was determined by measuring the resistance of the platinum thermometer with a Leeds and Northrup G-2 Mueller bridge, which

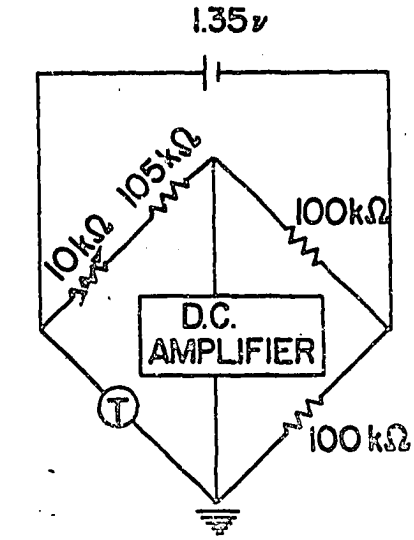

THERMOMETER CIRCUIT

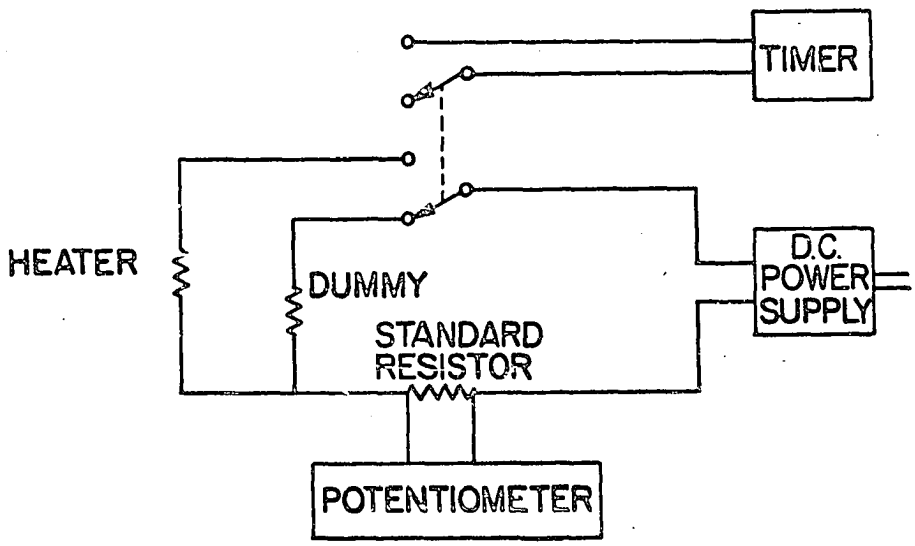

HEATER CIRCUIT

Figure 3. Calorimeter heater and thermometer circuits

had been calibrated against standard resistors in this laboratory. Simultaneously, the thermistor bridge was adjusted to bring the recorder pen as near as possible to the midpoint of the chart. Since the bridge could only be adjusted to the nearest ohm, and the resistance was required to 0.1 ohm, it was necessary to interpolate to obtain the final value. This procedure is easily understood when one realizes that the recorder served as nothing more than a recording galvanometer with the null point chosen as the midpoint of the chart. The calorimeter temperature and corresponding bridge reading were determined in this manner at intervals of 0.05°C. over the range 24.0 to 26.0°C. These results were fitted by the method of least squares to a polynomial of the form

$$\Theta = A + BR + CR^2 + DR^3 + ER^4 \qquad (4.1)$$

where Θ is the temperature in °C. and R is the bridge reading in ohms. In this method it is not necessary to know the actual thermistor resistance, which is the bridge reading plus about 105,000 ohms.

Calculation of the temperature from Equation 4.1 was simplified by making a table of temperature versus resistance at ten ohm intervals. An IBM 7074 computer was used to compute the table as well as to determine the least squares fit.

The thermistor was calibrated at the beginning of this work and again nine months later. During this time, the bridge was continuously energized and the thermistor was not subjected to mechanical or thermal shocks. The two calibra-

tions were found to differ by about 0.003°C. However, in this work we were only interested in the temperature difference between two resistance readings. A comparison of the two calibrations on this basis showed them to be identical to better than 5×10^{-5} °C.

7. Heater

The calorimeter heater (2-D) consisted of 63 inches of 38 B and S gauge, double silk covered manganin wire with two 30 B and S gauge copper leads. The wire was wound non-inductively in the threads of a thin-walled copper tube and annealed at 145°C. for 48 hours. After annealing, the heater resistance was 95.291 ohms, and periodic checks during the course of this work showed it to remain constant to within ± 0.002%.

The heater circuit is shown in Figure 3. Current for the heater was obtained from a constant current power supply, constructed by the Instrumentation Group of the Ames Laboratory. This power supply could be adjusted to give between 25 and 270 milliamperes current, which was constant to 0.005%. A dummy heater was used to allow the circuit to reach a steady operating condition. A Leeds and Northrup K-3 potentiometer was used to measure the potential drop across a 0.1 ohm standard resistor, thermostated at 25°C., in series with the heater. The standard resistor and standard cell used with the potentiometer were calibrated by the National Bureau of Standards. When the circuit was switched from the dummy heater to the calorimeter heater, an electronic timer was simultaneously activated. The

timer was calibrated to within 0.01 second against the National Bureau of Standards station WWV.

8. Adiabatic control

An eight junction copper-constantan thermopile was used to control the water bath at the temperature of the calorimeter. It was constructed from 36 B and S gauge copper wire and 32 B and S gauge constantan wire, which were silver soldered together and insulated with a light coat of varnish. The eight junctions in the bath were spaced at 3/4 inch intervals and placed in a copper tube (1-J). The other eight junctions were spaced at 1/4 inch intervals and placed in a tantalum well in the calorimeter (2-H). The thermopile wires, extending between the calorimeter and submarine lids, were housed in a 1/8 inch diameter, six mil wall, stainless steel tube (2-F). This tube was sealed to the two lids with Torr Seal and served as a vacuum tight conduit. Leads from the thermopile extended through a small hole in the stainless steel tube which was made vacuum right with Torr Seal.

The signal from the thermopile was fed to a phase sensitive, on-off type controller-amplifier, which was built by the Instrumentation Group of the Ames Laboratory. The controller also contained a recorder drive so the signal could be displayed on a strip-chart recorder. When the water bath was cooler than the calorimeter, the controller activated a 500 watt heater whose power output was controlled manually with a powerstat. The powerstat and cooling water were adjusted to

give nearly equal periods of heating and cooling of about 30 seconds duration. In this way the bath could be controlled to within $\pm$ 0.001°C. of the calorimeter and an adiabatic system obtained.

An auxilliary heater, capable of producing a maximum of 750 watts, was used in conjunction with the control heater during the period when the calorimeter temperature was raised. The power output of this heater was also manually regulated by a powerstat and was independent of the controller-amplifier.

When the control and auxilliary heater powerstats were properly adjusted, the bath temperature could be raised at the same rate as that of the calorimeter. During the ten minute heating period, deviations of the bath temperature from that of the calorimeter never exceeded $\pm$ 0.003°C. Furthermore, the control was such that the areas of positive and negative fluctuations were nearly equal and consequently, the net heat exchanged between the calorimeter and its surroundings was negligible. This can be shown to be true if we assume that heat transfer was by conduction and radiation, and the system obeyed Newton's Law of Cooling. These assumptions will be valid for the small temperature differences involved, so that

$$Q_u = -A \int (\theta - \theta_b) dt \qquad (4.2)$$

where Q_u is the net heat exchanged; A is the heat leak constant; $(\theta - \theta_b)$ is the difference between the calorimeter and bath temperatures; and t is the time. The integral in Equation 4.2 is the algebraic sum of the areas of positive and

negative temperature differences. Hence, Q_u will be a minimum when this sum is a minimum, i.e., when the two areas are equal.

The heat leak constant was determined by operating the calorimeter under isothermal conditions, and found to be 0.3 cal./°C./min. The integral in Equation 4.2 was evaluated by graphically integrating the differential temperature-time curve. Several determinations of Q_u were made, and it was found that the error in neglecting Q_u was less than 0.01% of the total energy input.

The success of this system was due to the fact that the temperature rise in the calorimeter was linear in time. In a reaction calorimeter, where the temperature rise due to a chemical reaction is not linear in time, Q_u may not be negligible, and a correction will have to be applied (62).

B. Experimental Procedure

1. Operation of the calorimeter

The following procedure was employed in all experimental measurements made with the calorimeter. The temperature of the water bath and the solution to be investigated were adjusted to approximately 24.0°C. A weighed amount of solution, whose volume was 105 ± 2 ml., was placed in the calorimeter vessel. Its weight was determined to one milligram and corrected to vacuum. After the apparatus was assembled, the submarine jacket was evacuated and the bath and calorimeter temperatures raised to 24.4°C. The bath control was regulated

so that adiabatic conditions were maintained, and approximately two hours were allowed for the system to reach equilibrium. By this time the pressure in the submarine jacket was of the order of 1×10^{-5} torr.

When equilibrium was established, the calorimeter temperature increased at a constant rate with time. The positive slope of the time-temperature curve was a result of the continuous energy input due to stirring. At the beginning of an experiment, one of the six available stirring speeds was selected which would give adequate mixing with the smallest possible slope. Experience showed this condition to be satisfied when the slope was about 2×10^{-5} °C./min. Since the heat of stirring was proportional to the stirring speed and the viscosity of the solution, slower speeds were employed for more concentrated solutions. However, throughout any particular experiment the same speed was used. The equilibration time of the system was not substantially reduced at the slower speeds because the thermal conductivity of the solutions also increased with increasing concentration.

When the fore slope of the time-temperature curve had been constant for at least 20 minutes, the current was switched from the dummy heater to the calorimeter heater, and the heating period begun. The current source had been previously adjusted so that the calorimeter temperature would be raised 0.4°C. in about ten minutes. During the heating period, the current flowing in the calorimeter heater was determined by

measuring the potential drop across the standard resistor. The amount of heat produced by the calorimeter heater, Q_e, was calculated from the relation

$$Q_e = \frac{1}{4.1840} \frac{R_h}{R_s^2} E_s^2 t , \qquad (4.3)$$

where Q_e is given in defined calories (1 calorie = 4.1840 absolute joules); R_h is the heater resistance; R_s is the resistance of the standard resistor (0.100037 ohms); E_s is the potential drop across the standard resistor; and t is the time in seconds that current flowed through the heater.

After the current was switched back to the dummy heater, the calorimeter temperature continued to rise to a maximum and then slowly decreased to the equilibrium value. The equilibration time was about 14 minutes. Once equilibrium was established, the calorimeter temperature again increased at a constant rate due to the heat of stirring.

The heat of stirring, Q_s, was evaluated from the slope of the time-temperature curve during the fore and after periods. The rate at which heat was added to the calorimeter by stirring was

$$\frac{dQs}{dt} = C_t \frac{d\theta}{dt} = g\, C_t , \qquad (4.4)$$

where $d\theta/dt = g$ is the slope of the time-temperature curve, and C_t is the heat capacity of the solution plus that of the calorimeter. Ideally the fore slope and after slope should have been identical, but in general, the after slope was slightly smaller. This was attributed to the lower viscosity

of the solution at the higher temperature. Consequently, the average of the fore and after slopes, $\bar{g}$, was used to compute an average heat of stirring, $\bar{Q}_s$. Substituting $\bar{g}$ into Equation 4.4 and integrating from t_i to t_f, the average heat of stirring was given by

$$\bar{Q}_s = C_t\, \bar{g}(t_f - t_i), \qquad (4.5)$$

where t_i was taken as the beginning of the heating period, and t_f as the time when the calorimeter temperature first reached equilibrium after the heating period.

In order to calculate the specific heat of a solution, the total energy input and the resulting temperature rise had to be determined. Since adiabatic conditions were maintained at all times, the net heat exchanged with the surroundings was zero, and the energy balance for the calorimeter between times t_i and t_f was

$$Q_e + Q_s = C_t(\theta_f - \theta_i), \qquad (4.6)$$

where θ_i is the calorimeter temperature at the beginning of the heating period, and θ_f is the calorimeter temperature when equilibrium was first established after the heating period. Substituting Equation 4.5 into Equation 4.6 gave the total heat capacity as

$$C_t = \frac{Q_e}{(\theta_f - \theta_i) - \bar{g}(t_f - t_i)}. \qquad (4.7)$$

The calorimeter temperatures were determined from Equation 4.1.

The heat capacity evaluated from Equation 4.7 was the sum of the heat capacities of the solution and the calorimeter.

The heat capacity of the solution was obtained by subtracting the heat capacity of the calorimeter. After correcting this value for the vaporization of solvent according to the method of Hoge (63), the result was the heat capacity of the solution under its saturated vapor pressure. The specific heat was found by dividing this result by the weight of the solution.

After the slope of the time-temperature curve had been constant for at least 15 minutes, a new heating period was started. This procedure was repeated three times in every experiment, giving three values for the specific heat of the solution in the temperature interval 24.4 to 25.6°C. These values usually agreed to better than 0.03%. The apparent molal heat capacity was computed from the average specific heat by means of Equation 2.27.

2. Heat capacity of the calorimeter

It was necessary to determine the heat capacity of the calorimeter before any solution measurements were made. This was done in the manner just described with the exception that a known weight of water was substituted for the solution. The heat capacity of the calorimeter was given by the difference between the heat capacity calculated from Equation 4.7, and the heat capacity of the water. A small correction for the vaporization of water was applied, and the heat capacity of the calorimeter was found to be 16.71 $\pm$ 0.02 cal./°C. This result was the average of 18 values. The specific heat of water was taken as 0.9989 cal./°C./gm. at 25°C. from the data

of Osborne et al. (64).

Periodic checks of this value were made and no variation was observed, provided the volume of water was the same. Although the difference was small, the heat capacity of the calorimeter was directly dependent on the amount of water used for the calibration. This was due to the indeterminate nature of the boundary of the calorimeter. As the volume of water in the calorimeter increased, the effective heat capacity of the calorimeter included a larger portion of the stainless steel hanger and stirring shaft. Rather than determine this volume dependence, the same amount of material was used in all solution measurements and calibrations, namely, 105 ± 2 ml.

3. Integrity of the calorimeter and method

In order to test the integrity of the calorimeter and the method employed in this work, the specific heat of several sodium chloride solutions was determined. This system had been studied by Randall and Rossini (38) using a differential calorimeter, and their results are reportedly accurate to 0.01%. Their specific heat data were converted to defined calories and fitted to a polynomial of third degree in molality by the method of least squares. Results of the measurements made in this work and their average deviation, and those of Randall and Rossini, calculated from the least squares polynomial expression, are given in Table 1.

A comparison of the two sets of measurements indicates that the method used in this research was capable of an

accuracy of at least 0.05%. This was also shown by the reproducibility obtained in those cases where several experiments were performed on the same rare-earth chloride solution.

Table 1. Specific heat of some sodium chloride solutions at 25°C.

Molality	Number of determinations	Specific heat	
		This research	Randall and Rossini (38)
0.45155	6	0.9665 ± 0.0002	0.9669
0.76647	9	0.9475 ± 0.0003	0.9477
0.81693	12	0.9448 ± 0.0003	0.9448
1.1246	3	0.9278 ± 0.0001	0.9280

C. Preparation of Solutions

The rare-earth chloride solutions were prepared by dissolution of the appropriate oxide in hydrochloric acid. The rare-earth oxides were obtained from the rare-earth separation group of the Ames Laboratory of the Atomic Energy Commission. Purity of the oxides was established by emission spectrographic analysis, and Table 2 shows the results of these analyses. The impurities are reported as the percent sesquioxide (monoxide in the case of calcium) present in the host.

Approximately two kilograms of rare-earth oxide were added to warm C.P. grade hydrochloric acid until the acid had completely reacted and a slight excess of the oxide remained. The solution was allowed to cool and the excess oxide removed

Table 2. Spectrographic analyses of rare-earth oxides

Oxide	Analysis[a] (percent)	
La_2O_3	Ce:	less than 0.03
	Pr:	less than 0.03
	Nd:	less than 0.02
	Fe:	less than 0.008
	Ca:	less than 0.01
Nd_2O_3	Pr:	less than 0.08
	Sm:	less than 0.10
	Fe:	less than 0.009
	Ca:	less than 0.04
Dy_2O_3	Gd:	less than 0.02
	Tb:	less than 0.10
	Ho:	less than 0.02
	Er:	less than 0.01
	Y:	less than 0.001
	Fe:	less than 0.01
	Ca:	less than 0.04
Er_2O_3	Dy:	less than 0.01
	Ho:	less than 0.005
	Tm:	less than 0.01
	Yb:	less than 0.005
	Y:	less than 0.001
	Fe:	less than 0.007
	Ca:	less than 0.02
Yb_2O_3	Er:	less than 0.005
	Tm:	less than 0.002
	Lu:	less than 0.003
	Y:	less than 0.01
	Fe:	less than 0.02
	Ca:	less than 0.02

[a]A result reported as "less than" reflects the lower limit of the analytical method. Therefore, the amount of impurity actually present may be much less than the value reported.

by filtration. A colloidal suspension of unreacted oxide remained after filtering and was dissolved by alternately adding small amounts of acid and gently heating. After a second filtration through a sintered glass funnel, the solution was basic in relation to the equivalence pH of the primary hydrolysis equilibrium

$$R^{+++} + H_2O \rightleftharpoons R(OH)^{++} + H^+ .$$

Several 25 milliliter aliquots of the solution were titrated with 0.05 N hydrochloric acid in order to determine its equilibrium pH. The titrations were performed with a Sargent Model D Recording Titrator using a glass pH indicating electrode and a calomel reference electrode. The equivalence pH was determined from the pH versus volume curve, and the stock solution was adjusted to this value with dilute hydrochloric acid. After heating the solution for several hours to dissolve any unreacted oxide, the pH was again measured and adjusted to the equivalence point. This procedure was repeated until no change in pH of the solution occurred upon heating.

The concentration of the stock solution was determined by two analyses; one for the rare-earth ion concentration, and another for the chloride ion concentration. For the rare earth analysis, a weighed amount of the stock solution was treated with a ten percent excess of a saturated solution of twice recrystallized oxalic acid. The precipitation was carried out in a porcelain crucible which had been brought to constant weight by ignition at 900°C. After evaporation to dryness

under infra-red lamps, the rare-earth oxalate was ignited to the oxide at 900°C. in a muffle furnace. From the weight of the oxide after ignition and the weight of the solution, the molality was calculated. Triplicate analyses were made and a precision of better than 0.05% obtained.

Lanthanum oxide is the most hygroscopic rare-earth oxide, and this property made it difficult to obtain satisfactory precision from the oxide analysis. Consequently, the lanthanum chloride stock solution was analyzed by precipitation of lanthanum sulfate with a slight excess of three molar sulfuric acid. The solution was slowly evaporated to dryness under heat lamps, and the excess sulfuric acid removed as sulfur trioxide by heating with a Meeker burner. Three samples were ignited in a muffle furnace at 700°C. and weighed as the sulfate. The precision obtained by this method was 0.03%.

A potentiometric method, employing a Sargent Model D Recording Titrator, was used in all chloride analyses. The electrode system consisted of a silver indicator electrode and a sleeve-type reference electrode with an ammonium nitrate bridge to the inner calomel electrode. About 50 grams of a 0.1 N standard silver nitrate solution was weighed into a beaker. Slightly more rare-earth chloride solution than necessary to react completely with the silver nitrate was added by weight to the beaker. The excess rare-earth solution was of such an amount that it could be titrated with one to five milliliters of standard silver nitrate using the recording

titrator to follow the course of the titration. From the total weight of standard silver nitrate solution and the weight of rare-earth chloride solution, the molality of the stock solution was calculated. The silver nitrate solution was standardized by titration of a sodium chloride solution, which had been prepared by weight. Triplicate analyses were made and the precision obtained was better than 0.05%.

Agreement between the rare earth and chloride analyses was about 0.1%, with the chloride analysis usually giving lower results. The average of the two analyses was taken as the concentration of the stock solution.

A series of dilutions, ranging in concentration from 0.1 molal to saturation, was prepared from known weights of stock solution and conductivity water. The conductivity water was obtained by distillation of regular distilled water from an alkaline potassium permanganate solution, and had a conductivity of less than 1×10^{-6} mhos per centimeter. All weights were corrected to weight in vacuum.

The saturated solutions were prepared by allowing about 500 milliliters of the stock solution to stand over magnesium perchlorate in a desiccator. After the solution was saturated, it was stored in a stoppered flask in a 25°C. water bath until needed. Before the solution was placed in the calorimeter, it was decanted away from the crystals and cooled to 24°C. Rare-earth solutions tend to supersaturate rather easily, so if they were not kept at this lower temperature

for more than a day, no new crystals formed, and the concentration remained at the 25°C. saturation value. Concentrations of the saturated solutions were taken from the data of Saeger and Spedding (5).

V. CALCULATIONS AND RESULTS

A. Treatment of the Data

Specific heats of aqueous solutions of lanthanum, neodymium, dysprosium, erbium, and ytterbium chloride were measured at 25°C. over the concentration range from 0.1 molal to saturation. The apparent molal heat capacity was calculated for each concentration from Equation 2.27,

$$\phi_{cp} = (\frac{1000}{m} + M_2)s - \frac{1000}{m} s^o. \qquad (2.27)$$

The specific heat of water was taken as 0.9989 cal./gm.°C. (64), and the molecular weights were computed from the atomic weight values reported in 1962 by Cameron and Wichers (65). From these values of the apparent molal heat capacity, an empirical equation of the form

$$\phi_{cp} = A + Bm^{1/2} + Cm + Dm^{3/2} + Em^2 \qquad (5.1)$$

was obtained for each salt by the method of least squares using an IBM 7074 computer. The apparent molal heat capacities were weighted by an amount inversely proportional to the square of their probable errors. The subject of probable errors is discussed later in this chapter.

An attempt was made to fit the data to an equation similar to Equation 5.1, with the exception that the parameter B was fixed at 89.9, the limiting slope predicted by the Debye-Hückel theory for aqueous 3-1 electrolytes (22). This procedure was unsuccessful because the expressions obtained did not adequately fit the experimental data at higher concentrations.

From Equations 5.1, 2.25, and 2.26; empirical equations of the form

$$\bar{C}_{p2} = A' + B'm^{1/2} + C'm + D'm^{3/2} + E'm^2 , \qquad (5.2)$$

and

$$\bar{C}_{p1} = 17.9955 + B''m^{3/2} + C''m^2 + D''m^{5/2} + E''m^3, \qquad (5.3)$$

were obtained for the partial molal heat capacities of the solute and solvent, respectively.

B. Tabulated Results

The experimental data and derived thermodynamic quantities for the five rare-earth chloride solutions studied in this work are summarized in Tables 3 through 13, and presented graphically in Figures 4 through 7. In all tables the concentration is expressed as the number of moles of solute per 1000 grams of water, the specific heat as defined calories per degree centigrade per gram of solution, and apparent and partial molal heat capacities as defined calories per degree centigrade per mole of solute. One defined calorie equals 4.1840 absolute joules.

The specific heats, s, and the apparent molal heat capacities, ϕ_{cp}, for the aqueous rare-earth chloride solutions are shown in Tables 3 through 7. The quantity Δ is the difference between the apparent molal heat capacity calculated from the least squares equation and that calculated from the specific heat. Variation of the specific heat with concentration for each of the rare-earth chloride solutions is shown graphically in Figure 4.

Table 3. Specific heats and apparent molal heat capacities of aqueous solutions of lanthanum chloride at 25°C.

m	$m^{\frac{1}{2}}$	s	$-\phi_{cp}$	$-\phi_{cp}$ [a] L.S.	Δ
0.10213	0.31958	0.9652	93.2	92.6	0.6
0.20139	0.44877	0.9350	88.1	86.4	1.7
0.29119	0.53962	0.9100	81.9	82.1	-0.2
0.40377	0.63543	0.8806	76.9	77.6	-0.7
0.49440	0.70314	0.8580	74.6	74.4	0.2
0.64686	0.80428	0.8236	69.1	69.4	-0.3
0.81024	0.90013	0.7902	63.8	64.4	-0.6
1.0076	1.0038	0.7531	59.2	58.8	0.4
1.2092	1.0996	0.7204	53.7	53.3	0.4
1.4108	1.1878	0.6917	48.1	48.0	0.1
1.6927	1.3010	0.6564	41.3	41.0	0.3
1.9750	1.4054	0.6276	34.0	34.3	-0.3
2.2517	1.5006	0.6031	27.9	28.1	-0.2
2.5649	1.6015	0.5792	21.6	21.6	0.0
2.8324	1.6830	0.5618	16.5	16.5	0.0
3.2896	1.8137	0.5364	9.0	8.9	0.1
3.6003	1.8974	0.5217	4.6	4.5	0.1
3.8959[b]	1.9738	0.5092	0.8	0.9	-0.1
				Average	±0.4

[a]Calculated from Equation 5.1 using the parameters in Table 11.

[b]Saturated solution.

Table 4. Specific heats and apparent molal heat capacities of aqueous solutions of neodymium chloride at 25°C.

m	$m^{\frac{1}{2}}$	s	$-\phi_{cp}$	$-\phi_{cp}$[a] L.S.	Δ
0.099586	0.31557	0.9657	91.4	94.4	-3.0
0.17264	0.41550	0.9428	88.7	89.0	-0.3
0.24320	0.50319	0.9189	85.7	84.6	1.1
0.35970	0.59975	0.8901	79.4	79.9	-0.5
0.49269	0.70192	0.8559	75.8	74.8	1.0
0.64067	0.80042	0.8223	69.6	69.9	-0.3
0.80080	0.89487	0.7886	65.0	64.9	0.1
1.0058	1.0029	0.7510	58.3	58.9	-0.6
1.2207	1.1048	0.7153	53.1	52.9	0.2
1.4553	1.2064	0.6824	46.5	46.6	-0.1
1.7024	1.3048	0.6518	40.6	40.1	0.5
1.9480	1.3957	0.6271	33.7	33.8	-0.1
2.2566	1.5022	0.6000	26.4	26.2	0.2
2.5524	1.5976	0.5796	19.0	19.2	-0.2
2.8974	1.7022	0.5600	11.2	11.3	-0.1
3.2499	1.8027	0.5436	3.9	3.8	0.1
3.5901	1.8948	0.5312	-2.8	-2.9	-0.1
3.9292[b]	1.9822	0.5214	-9.1	-9.1	0.0
				Average	±0.5

[a]Calculated from Equation 5.1 using the parameters in Table 11.

[b]Saturated solution.

Table 5. Specific heats and apparent molal heat capacities of aqueous solutions of dysprosium chloride at 25°C.

m	$m^{\frac{1}{2}}$	s	$-\phi_{cp}$	$-\phi_{cp}$[a] L.S.	Δ
0.097422	0.31213	0.9654	84.3	84.7	-0.4
0.16895	0.41104	0.9427	79.4	79.5	-0.1
0.24914	0.49914	0.9185	75.9	75.3	0.6
0.36080	0.60067	0.8872	71.1	70.7	0.4
0.49471	0.70336	0.8526	66.6	66.2	0.4
0.64312	0.80195	0.8179	61.6	61.8	-0.2
0.80745	0.89858	0.7826	57.5	57.3	0.2
1.0055	1.0028	0.7452	51.9	52.2	-0.3
1.2031	1.0969	0.7119	47.1	47.4	-0.3
1.4371	1.1988	0.6772	41.8	41.8	0.0
1.6767	1.2949	0.6464	36.4	36.3	0.1
1.9529	1.3975	0.6159	30.5	30.2	0.3
2.2620	1.5040	0.5878	23.7	23.8	-0.1
2.5342	1.5919	0.5661	18.6	18.7	-0.1
2.8530	1.6891	0.5440	13.2	13.2	0.0
3.1478	1.7742	0.5262	8.7	8.7	0.0
3.6310[b]	1.9055	0.4999	3.0	3.0	0.0
				Average	± 0.2

[a]Calculated from Equation 5.1 using the parameters in Table 11.

[b]Saturated solution.

Table 6. Specific heats and apparent molal heat capacities of aqueous solutions of erbium chloride at 25°C.

m	$m^{\frac{1}{2}}$	s	$-\phi_{cp}$	$-\phi_{cp}$[a] L.S.	Δ
0.10483	0.32378	0.9626	83.2	84.2	-1.0
0.17004	0.41236	0.9413	81.0	79.3	1.7
0.25090	0.50090	0.9169	75.9	74.9	1.0
0.36230	0.60191	0.8854	71.0	70.3	0.7
0.49531	0.70378	0.8509	65.9	65.9	0.0
0.64144	0.80090	0.8161	61.6	61.7	-0.1
0.77238	0.87885	0.7878	57.8	58.2	-0.4
1.0096	1.0048	0.7415	52.0	52.2	-0.2
1.2006	1.0957	0.7087	47.8	47.6	0.2
1.4609	1.2087	0.6704	41.4	41.5	-0.1
1.7153	1.3097	0.6381	35.8	35.7	0.1
1.9944	1.4122	0.6079	29.7	29.6	0.1
2.2695	1.5065	0.5824	24.1	24.0	0.1
2.5878	1.6087	0.5577	17.9	18.0	-0.1
2.9182	1.7083	0.5352	12.4	12.4	0.0
3.2497	1.8027	0.5158	7.5	7.7	-0.2
3.5379	1.8809	0.4995	4.5	4.4	0.1
3.7821[b]	1.9448	0.4868	2.2	2.2	0.0
				Average	±0.3

[a]Calculated from Equation 5.1 using the parameters in Table 11.

[b]Saturated solution.

Table 7. Specific heats and apparent molal heat capacities of aqueous solutions of ytterbium chloride at 25°C.

m	$m^{\frac{1}{2}}$	s	$-\phi_{cp}$	$-\phi_{cp}$[a] L.S.	Δ
0.10064	0.31724	0.9633	84.2	83.8	0.4
0.19779	0.44474	0.9321	77.4	77.7	-0.3
0.29215	0.54051	0.9035	74.2	73.4	0.8
0.38747	0.62247	0.8771	69.4	69.8	-0.4
0.49753	0.70536	0.8482	66.0	66.2	-0.2
0.65668	0.81036	0.8094	62.4	61.6	0.8
0.79439	0.89129	0.7802	57.3	57.8	-0.5
1.0046	1.0023	0.7390	52.2	52.4	-0.2
1.2056	1.0980	0.7044	47.5	47.5	0.0
1.4446	1.2019	0.6684	42.0	41.8	0.2
1.6772	1.2951	0.6383	36.7	36.5	0.2
1.9932	1.4118	0.6035	29.8	29.7	0.1
2.2579	1.5026	0.5789	24.3	24.3	0.0
2.5500	1.5969	0.5556	18.6	18.9	-0.3
2.8984	1.7025	0.5312	12.9	13.1	-0.2
3.2388	1.7997	0.5101	8.4	8.2	0.2
3.5154	1.8750	0.4949	5.1	5.0	0.1
4.0028[b]	2.0007	0.4702	0.7	0.8	-0.1
				Average	±0.3

[a]Calculated from Equation 5.1 using the parameters in Table 11.

[b]Saturated solution.

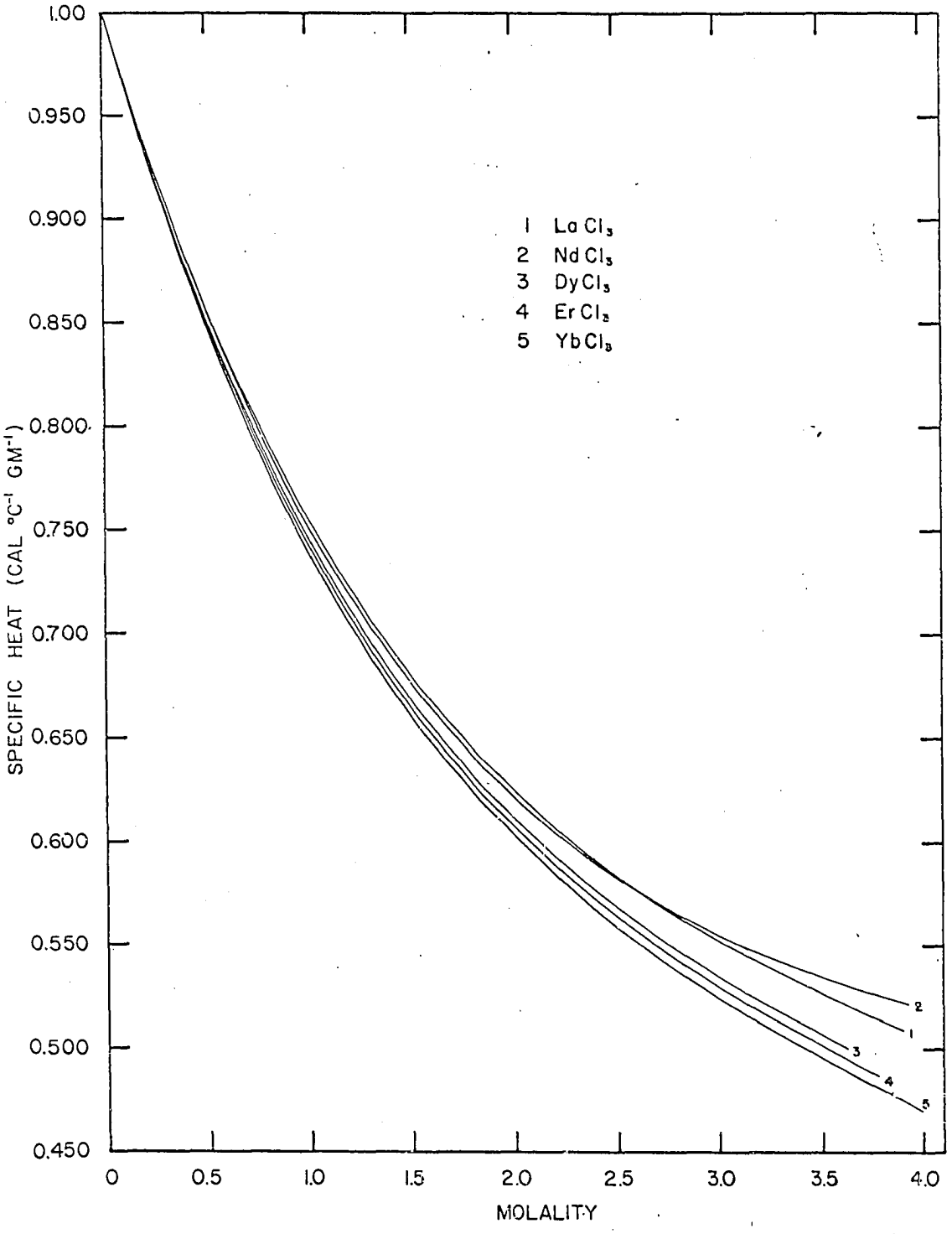

Figure 4. Specific heats of some aqueous rare-earth chloride solutions at 25°C.

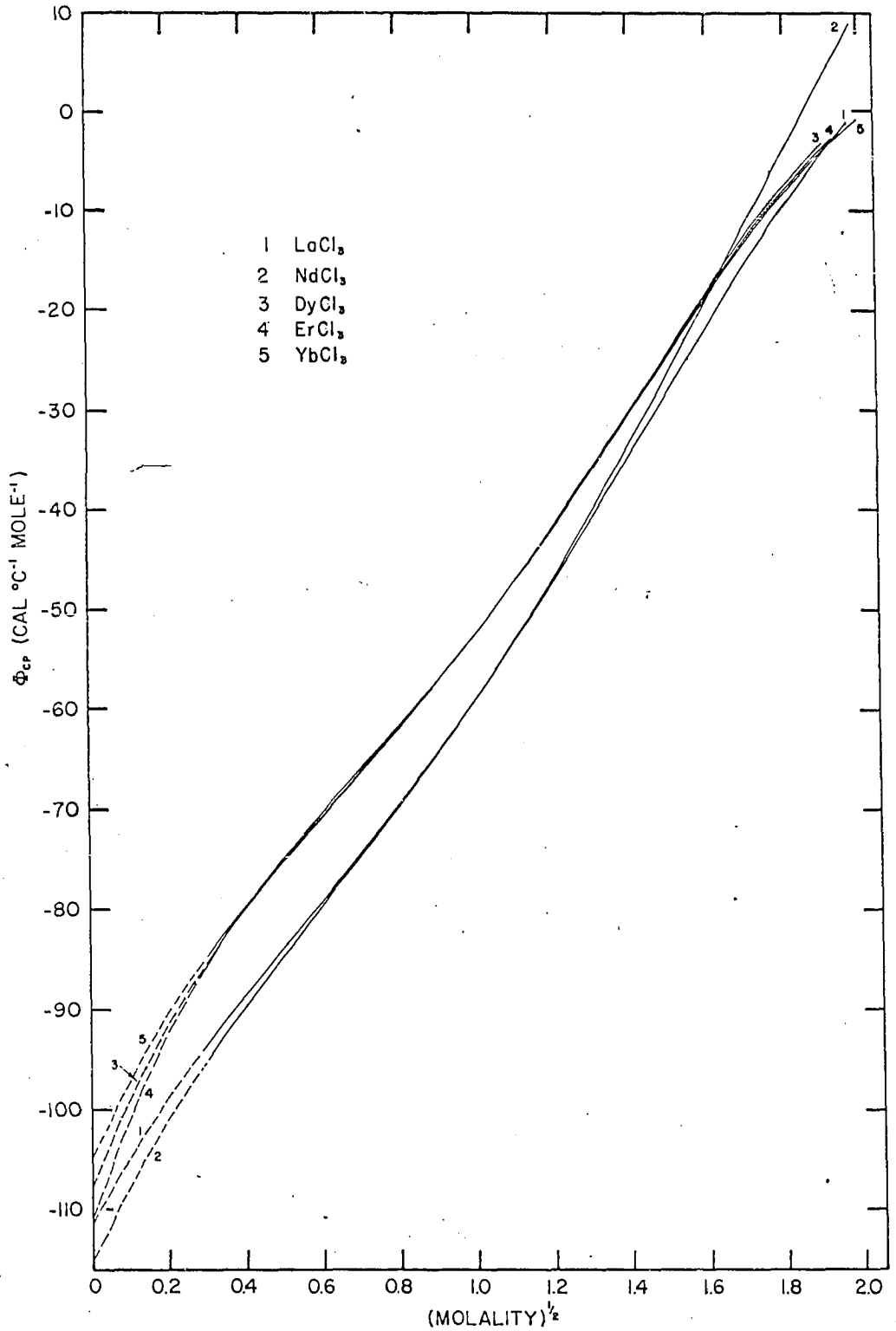

Figure 5. Apparent molal heat capacities of some aqueous rare-earth chloride solutions at 25°C.

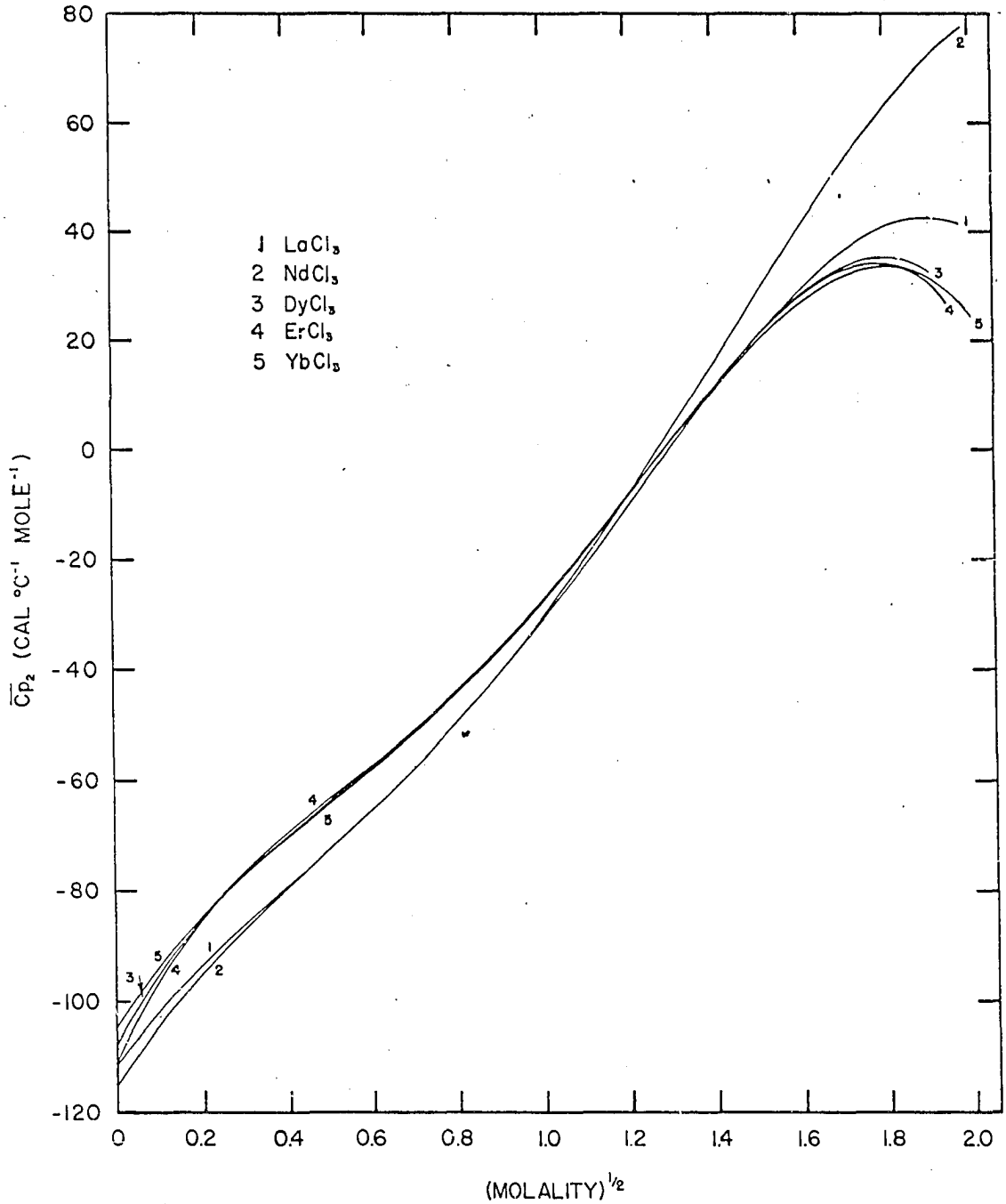

Figure 6. Partial molal heat capacities of the solute for some aqueous rare-earth chloride solutions at 25°C.

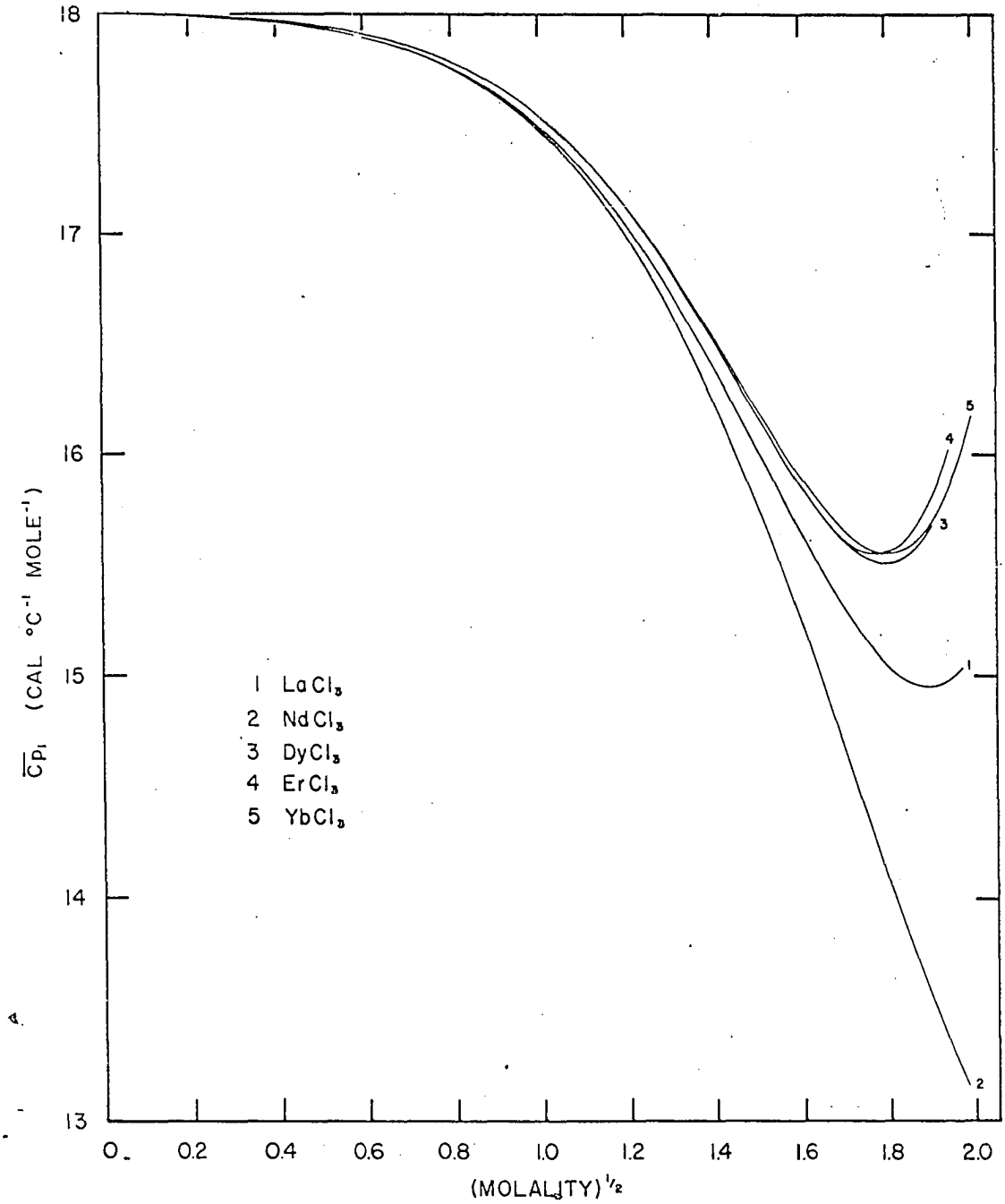

Figure 7. Partial molal heat capacities of water for some aqueous rare-earth chloride solutions at 25°C.

Table 8. Apparent molal heat capacities of rare-earth chloride solutions at 25°C in cal. $^{\circ}C^{-1}$ $mole^{-1}$

$m^{\frac{1}{2}}$	$-\phi_{cp}$[a]				
	$LaCl_3$	$NdCl_3$	$DyCl_3$	$ErCl_3$	$YbCl_3$
0.0	111.4[b]	115.1[b]	107.7[b]	110.9[b]	104.8[b]
0.3	93.6	95.2	85.4	85.6	84.7
0.4	88.7	89.8	80.0	79.9	79.7
0.5	84.0	84.8	75.2	74.9	75.2
0.6	79.3	79.9	70.7	70.4	70.8
0.7	74.5	74.9	66.3	66.0	66.5
0.8	69.6	69.9	61.9	61.7	62.0
0.9	64.4	64.6	57.3	57.2	57.4
1.0	59.0	59.1	52.4	52.4	52.5
1.1	53.3	53.2	47.2	47.4	47.4
1.2	47.3	47.0	41.7	42.0	41.9
1.3	41.0	40.4	36.0	36.3	36.2
1.4	34.6	33.5	30.1	30.4	30.4
1.5	28.2	26.4	24.1	24.4	24.5
1.6	21.7	19.0	18.2	18.5	18.7
1.7	15.5	11.5	12.6	12.8	13.2
1.8	9.6	4.0	7.5	7.8	8.2
1.9	4.3	-3.3	3.2	3.7	4.0
1.95	1.9	-6.8			2.4
2.0					0.8

[a]Calculated from Equation 5.1 using the parameters in Table 11.

[b]Obtained by extrapolation.

Table 9. Partial molal heat capacities of rare-earth chloride solutions at 25°C in cal. $^{\circ}C^{-1}$ $mole^{-1}$

$m^{\frac{1}{2}}$	$\bar{C}_{p2}$[a]				
	$LaCl_3$	$NdCl_3$	$DyCl_3$	$ErCl_3$	$YbCl_3$
0.0	-111.4	-115.1	-107.7	-110.9	-104.8
0.3	-86.0	-86.9	-76.8	-76.3	-76.8
0.4	-79.1	-79.5	-70.0	-69.3	-70.2
0.5	-72.3	-72.4	-63.7	-63.1	-64.0
0.6	-65.2	-65.1	-57.5	-57.2	-57.8
0.7	-57.6	-57.5	-51.0	-50.9	-51.2
0.8	-49.5	-49.3	-43.8	-44.1	-44.0
0.9	-40.6	-40.4	-35.9	-36.5	-36.1
1.0	-31.1	-30.6	-27.3	-27.9	-27.4
1.1	-21.0	-20.0	-17.9	-18.6	-18.1
1.2	-10.5	-8.6	-8.0	-8.6	-8.4
1.3	0.1	3.4	2.0	1.6	1.4
1.4	10.6	15.7	11.8	11.5	10.9
1.5	20.4	28.3	20.7	20.5	19.5
1.6	29.2	40.6	28.1	28.0	26.7
1.7	36.2	52.3	33.2	32.8	31.7
1.8	40.9	62.9	35.1	34.0	33.7
1.9	42.5	71.8	32.7	30.4	31.6
1.95	41.9	75.4			28.8
2.0					24.6

[a]Calculated from Equation 5.2 using the parameters in Table 12.

Table 10. Partial molal heat capacities of water in rare-earth chloride solutions at 25°C in cal.°C^{-1} mole^{-1}

$m^{\frac{1}{2}}$	$\bar{C}_{pl}$[a]				
	$LaCl_3$	$NdCl_3$	$DyCl_3$	$ErCl_3$	$YbCl_3$
0.0	17.9955	17.9955	17.9955	17.9955	17.9955
0.3	17.983	17.982	17.982	17.980	17.983
0.4	17.968	17.966	17.966	17.965	17.968
0.5	17.943	17.940	17.944	17.942	17.945
0.6	17.904	17.900	17.910	17.910	17.911
0.7	17.846	17.842	17.860	17.862	17.861
0.8	17.763	17.758	17.787	17.793	17.787
0.9	17.648	17.641	17.684	17.693	17.684
1.0	17.493	17.482	17.543	17.554	17.543
1.1	17.292	17.271	17.356	17.368	17.358
1.2	17.042	17.000	17.121	17.130	17.127
1.3	16.742	16.662	16.838	16.843	16.851
1.4	16.398	16.255	16.518	16.517	16.539
1.5	16.026	15.781	16.180	16.174	16.211
1.6	15.648	15.248	15.859	15.855	15.900
1.7	15.303	14.674	15.610	15.619	15.656
1.8	15.045	14.091	15.508	15.555	15.550
1.9	14.947	13.543	15.658	15.781	15.678
1.95	14.987	13.300			15.869
2.0					16.168

[a]Calculated from Equation 5.3 using the parameters in Table 13.

Table 11. Parameters for the empirical expressions of ϕ_{cp} corresponding to Equation 5.1

Salt	A	B	C	D	E
$LaCl_3$	-111.35	71.22	-52.453	44.768	-11.204
$NdCl_3$	-115.07	80.14	-59.044	44.626	-9.732
$DyCl_3$	-107.70	97.03	-94.920	69.738	-16.539
$ErCl_3$	-110.93	112.86	-118.806	83.889	-19.466
$YbCl_3$	-104.84	85.81	-79.761	61.075	-14.822

Table 12. Parameters for the empirical expressions of $\bar{C}_{p2}$ corresponding to Equation 5.2

Salt	A'	B'	C'	D'	E'
$LaCl_3$	-111.35	106.83	-104.906	111.920	-33.612
$NdCl_3$	-115.07	120.21	-118.088	111.565	-29.196
$DyCl_3$	-107.70	145.54	-189.840	174.345	-49.617
$ErCl_3$	-110.93	169.29	-237.612	209.722	-58.398
$YbCl_3$	-104.84	128.72	-159.522	152.688	-44.466

Table 13. Parameters for the empirical expressions of $\bar{C}_{p1}$ corresponding to Equation 5.3

Salt	B"	C"	D"	E"
$LaCl_3$	-0.64153	0.94496	-1.20977	0.40369
$NdCl_3$	-0.72187	1.06370	-1.20593	0.35065
$DyCl_3$	-0.87401	1.71002	-1.88453	0.59591
$ErCl_3$	-1.01660	2.14033	-2.26693	0.70137
$YbCl_3$	-0.77295	1.43692	-1.65043	0.53405

Values of ϕ_{cp}, $\bar{C}_{p2}$, and $\bar{C}_{p1}$, which were computed from the appropriate empirical equations, are given at rounded values of $m^{\frac{1}{2}}$ in Tables 8, 9, and 10, respectively. The parameters in the empirical equations are given for each salt in Tables 11, 12, and 13. Figures 5, 6, and 7 respectively show the variation of ϕ_{cp}, $\bar{C}_{p2}$, and $\bar{C}_{p1}$ with $m^{\frac{1}{2}}$.

C. Error Analysis

The apparent molal heat capacity is a derived quantity which is dependent on the experimentally measured specific heat and molal concentration of the solution. Consequently, any uncertainty in the apparent molal heat capacity is a result of uncertainties in these measured quantities.

The principle of propagation of precision indexes (66) provides a means whereby the probable error in a derived quantity can be estimated from the probable errors in the independently measured variables. Since the probable errors in the specific heat and concentration are independent, the propagation of these errors onto the apparent molal heat capacity is given by

$$P_{\phi_{cp}}^2 = \left(\frac{\partial \phi_{cp}}{\partial s}\right)^2 P_s^2 + \left(\frac{\partial \phi_{cp}}{\partial m}\right)^2 P_m^2 \quad , \qquad (5.4)$$

where $P_{\phi_{cp}}$ is the probable error in the apparent molal heat capacity; P_s, the probable error in the specific heat; and P_m, the probable error in the molal concentration.

Applying Equation 5.4 to the apparent molal heat capacity as expressed by Equation 2.27, one obtains

$$P^2_{\phi_{cp}} = \left[\frac{1000}{m} + M_2\right]^2 P_s^2 + \left[\frac{1000(s^o-s)}{m^2}\right]^2 P_m^2 . \qquad (5.5)$$

The probable error in the concentration was estimated from the precision of the chloride and rare-earth analyses to be less than 0.1%. The probable error in the specific heat was estimated from the precision of all specific heat measurements to be less than 5×10^{-4} cal./gm.^oC.

Table 14 shows the results of calculations of the probable error in the apparent molal heat capacity for solutions of ytterbium chloride investigated in this work. The individual contributions due to the estimated maximum errors in the specific heat and concentration are also shown. It is evident that the major source of error in the apparent molal heat capacity is from the uncertainty in the specific heat, and this contribution increases rapidly as the concentration decreases.

Table 14. Probable error in the apparent molal heat capacity for ytterbium chloride solutions

m	$m^{\frac{1}{2}}$	$-\phi_{cp}$	$\left\lvert\frac{\partial \phi_{cp}}{\partial s}\right\rvert P_s$	$\left\lvert\frac{\partial \phi_{cp}}{\partial m}\right\rvert P_m$	$P_{\phi_{cp}}$
0.10064	0.31724	84.2	5.11	0.35	5.1
0.19779	0.44474	77.4	2.67	0.34	2.7
0.29215	0.54051	74.2	1.85	0.32	1.9
0.38747	0.62247	69.4	1.43	0.31	1.5
0.49753	0.70536	66.0	1.14	0.30	1.2
0.65668	0.81036	62.4	0.90	0.29	1.0
0.79439	0.89129	57.3	0.77	0.28	0.8
1.0046	1.0023	52.2	0.64	0.26	0.7
1.2056	1.0980	47.5	0.55	0.24	0.6
1.4446	1.2019	42.0	0.48	0.23	0.5
1.6772	1.2951	36.7	0.44	0.22	0.5
1.9932	1.4118	29.8	0.39	0.20	0.4
2.2579	1.5026	24.3	0.36	0.19	0.4
2.5500	1.5969	18.6	0.34	0.17	0.4
2.8984	1.7025	12.9	0.31	0.16	0.4
3.2388	1.7997	8.4	0.29	0.15	0.3
3.5154	1.8750	5.1	0.28	0.14	0.3
4.0028	2.0007	0.7	0.26	0.13	0.3

VI. DISCUSSION

The data obtained in this research were concerned with solutions too concentrated to be expected to obey the Debye-Hückel limiting law. It must be emphasized that the parameters in the polynomial expressions for the apparent and partial molal heat capacities are completely empirical. They were computed to give the best fit of the experimental data at concentrations greater than 0.1 molal, and any interpretation based on an extrapolation of the polynomial equations outside this concentration range must be done with reservation. Furthermore, because of uncertainties in the first and second temperature derivatives of the dielectric constant of water, the presently accepted value of 89.9 for the limiting slope of the apparent molal heat capacity for 3-1 electrolytes (22) is subject to considerable uncertainty. Consequently, although the limiting slopes for the apparent molal heat capacity differ in some cases by as much as 25% from the accepted theoretical value, this does not imply that the rare-earth chlorides do not obey the Debye-Hückel theory. Indeed, there is ample evidence to the contrary (4,7). Similarly, the values reported for the apparent molal heat capacity at infinite dilution are subject to considerable uncertainty, perhaps as much as 10%. A direct comparison with the present study is impossible, but it is interesting to note that Jekel *et al.* (67) have reported a value of -104 $\pm$ 5 cal/mole ^{o}C. for the apparent molal heat capacity of gadolinium chloride at infinite dilution. The

corresponding value obtained in this work for dysprosium chloride was -107.7 cal./mole °C., and since one would not expect the two salts to be greatly different, the agreement is satisfactory.

The apparent molal heat capacity is generally negative for dilute aqueous solutions of strong electrolytes, and the rare-earth chlorides are no exception in this respect. A negative apparent molal heat capacity in dilute aqueous solutions can be explained on the basis of ion-solvent interactions. For example, a rare-earth ion, because of its high charge density, will interact strongly with the water molecules in the first hydration shell. Such interaction will considerably restrict certain rotational degrees of freedom of the water molecules, substantially reducing their contribution to the heat capacity of the solution. The orienting effect of the central ion will extend beyond the first hydration shell and cause a somewhat smaller loss in heat capacity of the water molecules in the outer shells too. In dilute solutions the loss in heat capacity of the oriented water molecules predominates over the heat capacity which may be ascribed to the ion-hydrates that are formed. Consequently, the heat capacity of a dilute electrolytic solution is less than that of the pure solvent, and the apparent molal heat capacity is negative. This is evident from its definition, viz.,

$$\phi_{cp} = \frac{C_p - n_1 \bar{C}^o_{p1}}{n_2} . \qquad (2.17)$$

The contribution of the ion-hydrates to the heat capacity of the solution will increase as the concentration increases, and the loss in heat capacity of the oriented water molecules will no longer be the predominant effect. Therefore, the difference between the heat capacity of the solution and that of the pure solvent will decrease, resulting in the apparent molal heat capacity becoming more positive with increasing concentration. As is shown in Figure 5, the apparent molal heat capacities of the rare-earth chlorides increase with concentration. All of the curves exhibit a slight S-shaped character, and except for neodymium, show a small decrease in slope near saturation.

The regular decrease in ionic radius across the rare-earth series, while maintaining the ionic charge constant, provides an excellent opportunity to investigate the effect of ion size on the apparent molal heat capacity. Due to the greater charge densities of the smaller rare-earth ions, one might expect the apparent molal heat capacity at low concentrations to decrease smoothly as the atomic number increases. It is evident from Figure 5 that this behavior was not observed. Instead, the apparent molal heat capacities of lanthanum and neodymium are less than those of dysprosium, erbium, and ytterbium. Furthermore, at all concentrations below 1.5 molal, the apparent molal heat capacities of lanthanum and neodymium are identical, within experimental error. Similarly, the apparent molal heat capacities of dysprosium,

erbium, and ytterbium are identical at all concentrations below 1.5 molal, within experimental error. These results indicate that a fundamental difference exists between the light and heavy rare earths which cannot be explained on the basis of ionic radius alone.

Substantial evidence has been accumulated in this laboratory by Dr. F. H. Spedding and his students which suggests that the observed differences in the solution properties of the rare-earth salts are due to a change in hydration of the rare-earth ions as the atomic number increases. For example, evidence for a difference in the water coordination number of the light and heavy rare-earth ions is provided by the apparent molal volume studies of Ayres (68) (4, p. 330); Saeger and Spedding (5); Spedding and Pikal[1]; and Spedding, Brown, and Gray[2]. These investigators found that as the atomic number increases, the apparent molal volumes of the rare-earth chlorides decrease from lanthanum to neodymium, then increase from neodymium to about gadolinium, and finally decrease throughout the remainder of the series. They postulated that the heavy rare-earth ions have a smaller coordination number

---

[1]Spedding, F. H. and Pikal, M. J., Ames Laboratory of the A.E.C., Ames, Iowa. Apparent molal volumes of some aqueous rare-earth chloride solutions at 25°C. Private communication. 1964.

[2]Spedding, F. H., Brown, M. and Gray, K., Ames Laboratory of the A.E.C., Ames, Iowa. Apparent molal volumes of some aqueous rare-earth chloride solutions at 25°C. Private communication. 1964.

than do the light rare-earth ions; and that an equilibrium existed between the two coordination numbers for the ions between neodymium and gadolinium. Moreover, they suggested that the equilibrium shifted toward the smaller coordination number as the concentration increased for the ions between neodymium and gadolinium. Csejka and Spedding (6) and DeKock (7) have observed very similar behavior for the relative apparent molal enthalpies of the rare-earth chloride solutions.

Additional evidence for the existence of two subgroups within the rare-earth series is given by the studies of the heat of formation of rare-earth chelates by Mackey et al. (69) and Grenthe (70). These authors agree that their results cannot be explained by ligand-field stabilization of the 4-f orbitals, but are probably due to a change in hydration of the rare-earth ions near the middle of the series.

The data obtained in this research can be qualitatively explained on the basis of a decrease in the number of water molecules in the first hydration shell of the rare-earth ions as the ionic radii decrease. A lower coordination number for the smaller ions implies a larger amount of un-coordinated water in the solution per mole of solute. Since this un-coordinated water will have a larger heat capacity than it had in the hydration shell of the ion, a more positive apparent molal heat capacity will result for the smaller rare-earth ions. This is precisely what is observed at concentrations less than 1.5 molal; however, at higher concentrations, the

apparent molal heat capacity of neodymium chloride begins to increase rapidly compared to the other four salts. This apparently anomalous behavior suggests that an equilibrium exists between neodymium ions with two coordination numbers, but that in the other rare-earth solutions investigated in this work, such an equilibrium does not exist; at least not to any appreciable extent. As the concentration increases, the equilibrium shifts to a higher percentage of neodymium ions with a lower coordination number. Such a shift in equilibrium would lead to a sharper rise in the apparent molal heat capacity of neodymium chloride relative to the other rare-earth chlorides.

There is ample evidence to support the hypothesis that a change in coordination number occurs within the rare-earth series. The structural studies of Helmholz (71) give a coordination number of nine for water about the neodymium ion in $Nd(BrO_3)_3 \cdot 9H_2O$, while those Marezio et al. (72) give a value of eight for gadolinium, six water molecules and two chloride ions, in $GdCl_3 \cdot 6H_2O$. Proton relaxation data obtained on aqueous gadolinium perchlorate solutions led Morgan (73) to predict an equal probability of either eight or nine as the coordination number of gadolinium. On the basis of spectroscopic studies of aqueous europium chloride solutions, Miller (74) proposed that the close-in water configuration around the trivalent europium ion was that of the eight water molecules in the ice III structure. Furthermore, he suggested

that this structure was the most probable one for all rare-earth ions smaller than europium, but expected considerable distortion of the ice III lattice with the larger rare earths. While these studies do not prove that a change in hydration occurs in aqueous rare-earth solutions, they lend credence to the possibility of such behavior.

It is impossible at the present time to give a definitive interpretation of the behavior of the apparent and partial molal heat capacities at high concentrations. However, it is expected that a number of factors will be manifesting themselves near saturation which were unimportant or essentially lacking in more dilute solutions. For example, complex-ion formation and ion-pair formation can be reasonably expected to occur in very concentrated solutions. Structural studies of Marezio et al. (72) have shown that gadolinium chloride hexahydrate consists of complexes of the type $\left[Cl_2Gd(OH_2)_6\right]^+$. Interpretation of the behavior of solutions on the basis of crystal structure evidence is at best an approximation, but it is reasonable to assume that similar complex units also exist in nearly saturated solutions. From Figures 6 and 7, it is evident that the partial molal heat capacities of lanthanum, dysprosium, erbium, and ytterbium chloride solutions exhibit a marked change in slope near saturation, and it is possible that such behavior reflects the influence of complex species on the heat capacity of the solutions. The lack of a marked slope change in the partial molal heat capacity of neodymium

chloride is attributed to a competition between two effects; the coordination number equilibrium discussed above and complex-ion formation, with the former exerting the predominant influence on the heat capacity of the solution.

A quantitative interpretation of the results obtained in this research will have to await a more precise knowledge of the species present in the solutions. Additional studies of the heat capacities of other rare-earth chloride solutions are under way in this laboratory at the present time. These studies should help to clarify the explanations given above. On the basis of the results obtained in the present work, one would expect dilute solutions of the chlorides of samarium, europium, and gadolinium to exhibit apparent molal heat capacity values intermediate to those of neodymium and dysprosium. At higher concentrations, praseodymium and samarium are expected to show behavior similar to neodymium, as a result of the shift in equilibrium of their water coordination numbers.

VII. SUMMARY

An adiabatic calorimeter was designed and built to measure the specific heats of aqueous solutions at 25°C. with a precision of at least 0.05%. The apparatus consisted of a calorimeter vessel suspended in a submarine jacket, which was submerged in a well stirred water bath. In order to minimize heat transfer, the submarine jacket was evacuated and adiabatic conditions were maintained between the calorimeter vessel and its surroundings. An eight junction copper-constantan thermopile between the calorimeter vessel and the water bath served as a differential temperature sensing device for the adiabatic controller. The calorimeter temperature was continuously monitored by recording the output of a Wheatstone bridge circuit, employing a 100,000 ohm thermistor as the temperature sensing device. To ensure chemical inertness, tantalum was used for all parts of the calorimeter which came into contact with the solution.

Specific heats were determined for a number of aqueous solutions of lanthanum, neodymium, dysprosium, erbium, and ytterbium chlorides at 25°C. The concentration range covered was from 0.1 molal to saturation (approximately 4.0 molal). From the specific heat data, apparent molal heat capacities were calculated for each of the rare-earth chloride solutions. The apparent molal heat capacity results for each salt were expressed as a function of the square root of molality by

means of a fourth degree polynomial equation. Partial molal heat capacities of the solute and solvent were calculated for each rare-earth salt from these polynomial equations.

The apparent molal heat capacity data obtained in this investigation indicate the rare earths may be divided into two subgroups at moderate concentrations, with the heavy rare earths belonging to one group and the light rare earths to another. This behavior was qualitatively explained by assuming that the heavy rare-earth ions have a lower coordination number for water than the light ones, and evidence to support this assumption was presented. At higher concentrations neodymium behaved more like a heavy rare earth than a light one. This was attributed to the existence of an equilibrium between two water coordination numbers for the neodymium ion, with the equilibrium shifting towards the smaller coordination number as the concentration increased. The partial molal heat capacities showed possible evidence for complex-ion formation near saturation.

VIII. BIBLIOGRAPHY

1. Debye, P. and Hückel, E., Physik. Z., 24, 185 (1923).

2. Lewis, G. N., Proc. Am. Acad. Arts Sci., 43, 259 (1907).

3. Powell, J. E., "Separation of the Rare Earths by Ion Exchange". In Spedding, F. H. and Daane, A. H., eds., "The Rare Earths", pp. 55-73, John Wiley and Sons, Inc., New York, N.Y., 1961.

4. Spedding, F. H. and Atkinson, Gordon, "Properties of Rare Earth Salts in Electrolytic Solutions". In Hamer, Walter J., ed., "The Structure of Electrolytic Solutions", pp. 319-339, John Wiley and Sons, Inc., New York, N.Y., 1959.

5. Saeger, V. W. and Spedding, F. H., U.S. Atomic Energy Commission Report, IS-338 (Iowa State University of Science and Technology, Ames, Iowa. Institute for Atomic Research) (1960).

6. Csejka, D. A. and Spedding, F. H., U.S. Atomic Energy Commission Report, IS-417 (Iowa State University of Science and Technology, Ames, Iowa. Institute for Atomic Research) (1961).

7. De Kock, Carroll W., "Heats of Dilution of Some Aqueous Rare-Earth Chloride Solutions at 25°C.", unpublished Ph.D. thesis, Library, Iowa State University of Science and Technology, Ames, Iowa, 1965.

8. Arrhenius, S., Z. physik. Chem., 1, 631 (1887).

9. van't Hoff, J. H., Z. physik. Chem., 1, 481 (1887).

10. van Laar, J. J., Z. physik. Chem., 15, 457 (1894).

11. Sutherland, W., Phil. Mag., 3, 167 (1902).

12. Sutherland, W., Phil. Mag., 7, 1 (1906).

13. Bjerrum, N., Z. Electrochem., 24, 321 (1918).

14. Milner, R., Phil. Mag., 23, 551 (1912).

15. Milner, R., Phil. Mag., 25, 742 (1913).

16. Kramers, H. A., Proc. Acad. Sci. Amsterdam, 30, 145 (1927).

17. Fowler, R. H., Trans. Faraday Soc., 23, 434 (1927).

18. Onsager, L., Chem. Rev., 13, 73 (1933).

19. Kirkwood, J. G., J. Chem. Phys., 2, 767 (1934).

20. Fowler, R. and Guggenheim, E. A., "Statistical Thermodynamics", Cambridge University Press, Cambridge, England, 1960.

21. Kirkwood, J. G. and Poirier, J. C., J. Phys. Chem., 58, 591 (1954).

22. Harned, H. S. and Owen, B. B., "The Physical Chemistry of Electrolytic Solutions", 3rd ed., Reinhold Publishing Corporation, New York, N.Y., 1958.

23. Robinson, R. A. and Stokes, R. H., "Electrolyte Solutions", 2nd ed., Butterworths Scientific Publications, London, England, 1959.

24. Bjerrum, N., Kgl. Danske Vidensk. Selskab., 7, No. 9 (1926). Original available but not translated; cited in Harned, H. S. and Owen, B. B., "The Physical Chemistry of Electrolytic Solutions", 3rd ed., p. 70, Reinhold Publishing Corporation, New York, N.Y., 1958.

25. Fuoss, R. M. and Kraus, C. A., J. Am. Chem. Soc., 55, 2387 (1933).

26. Fuoss, R. M. and Kraus, C. A., J. Am. Chem. Soc., 57, 1 (1935).

27. Hückel, E., Physik. Z., 26, 93 (1925).

28. Scatchard, G., Chem. Rev., 19, 309 (1936).

29. Stokes, R. H. and Robinson, R. A., J. Am. Chem. Soc., 70, 1870 (1948).

30. Glueckauf, E., Trans. Faraday Soc., 51, 1235 (1955).

31. Gronwall, T. H., La Mer, V. K., and Sandved, K., Physik. Z., 29, 358 (1928).

32. La Mer, V. K., Gronwall, T. H., and Greiff, L. J., J. Phys. Chem., 35, 2245 (1931).

33. Eigen, M. and Wicke, E., J. Phys. Chem., 58, 702 (1954).

34. Wicke, E. and Eigen, M., Z. Electrochem., 56, 551 (1952).

35. Mayer, J. E., J. Chem. Phys., 18, 1426 (1950).

36. Poirier, J. C., J. Chem. Phys., 21, 972 (1953).

37. Randall, M. and Ramage, W. D., J. Am. Chem. Soc., 49, 93 (1927).

38. Randall, M. and Rossini, F. D., J. Am. Chem. Soc., 51, 323 (1929).

39. Gucker, F. T. and Schminke, K. H., J. Am. Chem. Soc., 54, 1358 (1932).

40. Gucker, F. T. and Schminke, K. H., J. Am. Chem. Soc., 55, 1013 (1933).

41. Gucker, F. T., Ayres, F. D., and Rubin, T. R., J. Am. Chem. Soc., 58, 2118 (1936).

42. Rossini, F. D., J. Research Natl. Bur. Standards, 7, 47 (1931).

43. La Mer, V. K. and Cowperthwaite, I. A., J. Am. Chem. Soc., 55, 1004 (1933).

44. Young, T. F. and Machin, J. S., J. Am. Chem. Soc., 58, 2254 (1936).

45. Wallace, W. E. and Robinson, A. L., J. Am. Chem. Soc., 63, 958 (1941).

46. Robinson, A. L. and Wallace, W. E., Chem. Rev., 30, 195 (1942).

47. Spedding, F. H. and Miller, C. F., J. Am. Chem. Soc., 74, 3158 (1952).

48. Zwicky, F., Physik. Z., 26, 664 (1925).

49. Zwicky, F., Physik. Z., 27, 271 (1926).

50. Zwicky, F., Proc. Natl. Acad. Sci. U.S., 12, 86 (1926).

51. Gucker, F. T., Chem. Rev., 13, 111 (1933).

52. Everett, D. H. and Coulson, C. A., Trans. Faraday Soc., 36, 633 (1940).

53. Fuoss, R. M. and Onsager, L., Proc. Natl. Acad. Sci. U.S., 47, 818 (1961).

54. White, W. P., "The Modern Calorimeter", The Chemical Catalog Company, Inc., New York, N.Y., 1928.

55. Swietoslawski, W., "Microcalorimetry", Reinhold Publishing Corporation, New York, N.Y., 1946.

56. Sturtevant, J. M., "Calorimetry", in Weissberger, Arnold, ed., "Technique of Organic Chemistry", 3rd ed., Vol. 1, Part 1, pp. 523-654, Interscience Publishers, Inc., New York, N.Y., 1959.

57. Skinner, H. A., "Experimental Thermochemistry", Vol. 2, Interscience Publishers, Inc., New York, N.Y., 1962.

58. Argue, G. R., Mercer, E. E., and Cobble, J. W., J. Phys. Chem., 65, 2041 (1961).

59. Vanderzee, C. E. and Myers, R. A., J. Phys. Chem., 65, 153 (1961).

60. Fitzgibbon, G. C., Pavone, D., Huber, E. J., and Holley, C. E., U.S. Atomic Energy Commission Report, LA-3031 (Los Alamos Scientific Laboratory, Los Alamos, New Mexico) (1964).

61. Sunner, S. and Wadsö, I., Acta Chem. Scand., 13, 97 (1959).

62. Dole, M., Hettinger, W. P., Larson, N., Wethington, J. A., and Worthington, A. E., Rev. Sci. Instr., 22, 812 (1951).

63. Hoge, H. J., J. Research Natl. Bur. Standards, 36, 111 (1946).

64. Osborne, N. S., Stimson, H. F., and Ginnings, D. J., J. Research Natl. Bur. Standards, 23, 197 (1939).

65. Cameron, A. E. and Wichers, E., J. Am. Chem. Soc., 84, 4175 (1962).

66. Worthing, A. G. and Geffner, J., "Treatment of Experimental Data", John Wiley and Sons, Inc., New York, N.Y., 1943.

67. Jekel, E. C., Criss, C. M., and Cobble, J. W., J. Am. Chem. Soc., 86, 5404 (1964).

68. Ayres, Buell O., "Apparent and Partial Molal Volumes of Some Rare Earth Salts in Aqueous Solutions", unpublished Ph.D. thesis, Library, Iowa State University of Science and Technology, Ames, Iowa, 1954.

69. Mackey, J. L., Powell, J. E., and Spedding, F. H., J. Am. Chem. Soc., 84, 2047 (1962).

70. Grenthe, I., Acta Chem. Scand., 17, 2487 (1963).

71. Helmholz, L., J. Am. Chem. Soc., 61, 1544 (1939).

72. Marezio, M., Plettinger, H. A., and Zachariasen, W. H., Acta Cryst., 14, 234 (1961).

73. Morgan, L. O., J. Chem. Phys., 38, 2788 (1963).

74. Miller, D. G., J. Am. Chem. Soc., 80, 3576 (1958).

IX. ACKNOWLEDGEMENTS

The author wishes to express his appreciation to Dr. F. H. Spedding for his encouragement, guidance, and patience throughout the course of this research and in the preparation of this thesis. Special thanks are extended to Dr. C. W. DeKock for many valuable discussions of calorimetric techniques; to Dr. P. T. Dawson for suggestions in the design of the vacuum system; and to Mr. Lael Smith and Mr. Harvey Meyer for assistance in building the calorimeter. Appreciation is also extended to all of the author's associates for their cooperation, comments, and moral support throughout the course of this work.